

Fermionic Molecular Dynamics



FMD Wave Functions

Nucleon-Nucleon Interaction

Mean-Field Calculations

**Projection After Variation and
Variation After Projection**

Fermionic

Slater determinant

$$|Q\rangle = \mathcal{A}\left(|q_1\rangle \otimes \cdots \otimes |q_A\rangle\right)$$

- antisymmetrized A -body state

Molecular

single-particle states

$$\langle \mathbf{x} | q \rangle = \sum_i c_i \exp\left\{-\frac{(\mathbf{x} - \mathbf{b}_i)^2}{2a_i}\right\} \otimes |\chi_i^\uparrow, \chi_i^\downarrow\rangle \otimes |\xi\rangle$$

- Gaussian wave-packets in phase-space (complex parameter \mathbf{b}_i encodes mean position and mean momentum), spin is free, isospin is fixed
- width a_i is an independent variational parameter for each wave packet
- superposition of two wave packets for each single particle state

Gaussian Wave Packets

- Wave Packet

$$\langle \mathbf{x} | a, \mathbf{b} \rangle = \exp \left\{ -\frac{(\mathbf{x} - \mathbf{b})^2}{2a} \right\}$$

- Norm

$$\langle a, \mathbf{b} | a, \mathbf{b} \rangle = \left(2\pi \frac{a^* a}{a^* + a} \right)^{3/2} \exp \left\{ -\frac{(\mathbf{b}^* - \mathbf{b})^2}{2(a^* + a)} \right\}$$

- Mean Position, Mean Momentum

$$\frac{\langle a, \mathbf{b} | \tilde{x} | a, \mathbf{b} \rangle}{\langle a, \mathbf{b} | a, \mathbf{b} \rangle} = \frac{a^* \mathbf{b} + a \mathbf{b}^*}{a^* + a}, \quad \frac{\langle a, \mathbf{b} | \tilde{k} | a, \mathbf{b} \rangle}{\langle a, \mathbf{b} | a, \mathbf{b} \rangle} = i \frac{\mathbf{b}^* - \mathbf{b}}{a^* + a}$$

- Variance of Position and Momentum

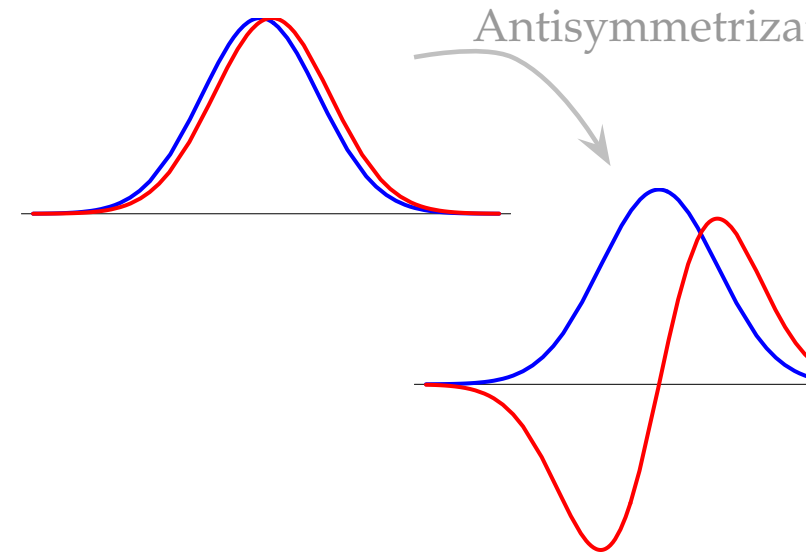
$$\frac{\langle a, \mathbf{b} | (\tilde{x} - \langle \tilde{x} \rangle)^2 | a, \mathbf{b} \rangle}{\langle a, \mathbf{b} | a, \mathbf{b} \rangle} = 3 \frac{a^* a}{a^* + a} \quad \frac{\langle a, \mathbf{b} | (\tilde{k} - \langle \tilde{k} \rangle)^2 | a, \mathbf{b} \rangle}{\langle a, \mathbf{b} | a, \mathbf{b} \rangle} = 3 \frac{1}{a^* + a}$$

Gaussian Wave Packets and Harmonic Oscillator

- Slater determinant invariant under linear transformation of single-particle states
- Harmonic Oscillator wave functions can be obtained by linear combinations of Gaussians
- Create s - and p -wave Harmonic Oscillator wave functions with two slightly shifted Gaussians

$$\lim_{\Delta \rightarrow 0} \frac{1}{2} (\langle x | a, +\Delta \rangle + \langle x | a, -\Delta \rangle) = \langle x | a, 0 \rangle$$

$$\lim_{\Delta \rightarrow 0} \frac{1}{2\Delta} (\langle x | a, +\Delta \rangle - \langle x | a, -\Delta \rangle) = x \langle x | a, 0 \rangle$$



Time-dependent

Time-dependent variational principle

$$\delta \int dt \frac{\langle Q | i \frac{d}{dt} - \hat{H} | Q \rangle}{\langle Q | Q \rangle} = 0$$

➤ describe heavy-ion reactions

Time-independent

Ritz variational principle

$$\delta \frac{\langle Q | \hat{H} - \hat{T}_{\text{cm}} | Q \rangle}{\langle Q | Q \rangle} = 0$$

➤ minimize expectation value with respect to all the parameters $q_k = \{c_k, a_k, \mathbf{b}_k, \chi_k\}$, $k = 1 \dots A$

➤ need analytical gradients

$$\frac{\partial}{\partial q_i} \frac{\langle Q | \hat{H} - \hat{T}_{\text{cm}} | Q \rangle}{\langle Q | Q \rangle}$$

Non-Orthogonal Basis

- Slater determinant is the antisymmetrized product state

$$\begin{aligned}
 |Q\rangle &= \tilde{\mathcal{A}}(|q_1\rangle \otimes \cdots \otimes |q_A\rangle) \\
 &= \frac{1}{A!} \sum_{\mathcal{P}} (-1)^{\mathcal{P}} (|q_{\mathcal{P}(1)}\rangle \otimes \cdots \otimes |q_{\mathcal{P}(A)}\rangle)
 \end{aligned}$$

- Antisymmetrization operator is a projection operator

$$\tilde{\mathcal{A}}\tilde{\mathcal{A}} = \tilde{\mathcal{A}}$$

- Many-Body Overlap

$$\begin{aligned}
 \langle Q|Q\rangle &= \left(\langle q_1| \otimes \cdots \otimes \langle q_A| \right) \tilde{\mathcal{A}}^\dagger \tilde{\mathcal{A}} (|q_1\rangle \otimes \cdots \otimes |q_A\rangle) \\
 &= \left(\langle q_1| \otimes \cdots \otimes \langle q_A| \right) \tilde{\mathcal{A}} (|q_1\rangle \otimes \cdots \otimes |q_A\rangle) \\
 &= \left(\langle q_1| \otimes \cdots \otimes \langle q_A| \right) \frac{1}{A!} \sum_{\mathcal{P}} (-1)^{\mathcal{P}} (|q_{\mathcal{P}(1)}\rangle \otimes \cdots \otimes |q_{\mathcal{P}(A)}\rangle) \\
 &= \det(\langle q_k|q_l\rangle)
 \end{aligned}$$

Evaluation of Matrix Elements

➔ non-orthogonal basis, use inverse overlap matrix

One-Body Matrix Elements

$$\frac{\langle Q | \tilde{O}^{[1]} | Q \rangle}{\langle Q | Q \rangle} = \sum_{k,l} \langle q_k | \tilde{O}^{[1]} | q_l \rangle o_{lk}$$

Two-body operators

$$\frac{\langle Q | \tilde{O}^{[2]} | Q \rangle}{\langle Q | Q \rangle} = \frac{1}{2} \sum_{k,l,m,n} \langle q_k, q_l | \tilde{O}^{[2]} | q_m, q_n \rangle (o_{mk} o_{nl} - o_{ml} o_{nk})$$

$$o = n^{-1} = \left(\langle q_i | q_j \rangle \right)^{-1}$$

Interaction Matrix Elements

(One-body) Kinetic Energy

$$\langle q_k | \tilde{T} | q_l \rangle = \langle a_k \mathbf{b}_k | \tilde{T} | a_l \mathbf{b}_l \rangle \langle \chi_k | \chi_l \rangle \langle \xi_k | \xi_l \rangle$$

$$\langle a_k \mathbf{b}_k | \tilde{T} | a_l \mathbf{b}_l \rangle = \frac{1}{2m} \left(\frac{3}{a_k^* + a_l} - \frac{(\mathbf{b}_k^* - \mathbf{b}_l)^2}{(a_k^* + a_l)^2} \right) R_{kl}$$

(Two-body) Potential

➔ fit radial dependencies by (a sum of) Gaussians

$$G(\mathbf{x}_1 - \mathbf{x}_2) = \exp\left\{-\frac{(\mathbf{x}_1 - \mathbf{x}_2)^2}{2\kappa}\right\}$$

➔ perform Gaussian integrals

$$\langle a_k \mathbf{b}_k, a_l \mathbf{b}_l | \tilde{G} | a_m \mathbf{b}_m, a_n \mathbf{b}_n \rangle = R_{km} R_{ln} \left(\frac{\kappa}{\alpha_{klmn} + \kappa} \right)^{3/2} \exp\left\{-\frac{\rho_{klmn}^2}{2(\alpha_{klmn} + \kappa)}\right\}$$

➔ analytical formulas for matrix elements

$$\alpha_{klmn} = \frac{a_k^* a_m}{a_k^* + a_m} + \frac{a_l^* a_n}{a_l^* + a_n}$$

$$\rho_{klmn} = \frac{a_m \mathbf{b}_k^* + a_k^* \mathbf{b}_m}{a_k^* + a_m} - \frac{a_n \mathbf{b}_l^* + a_l^* \mathbf{b}_n}{a_l^* + a_n}$$

$$R_{km} = \langle a_k \mathbf{b}_k | a_m \mathbf{b}_m \rangle$$

Operator Representation of V_{UCOM}

$$\tilde{C}^\dagger(\tilde{T} + \tilde{V})\tilde{C} = \tilde{T}$$

$$+ \sum_{ST} \hat{V}_c^{ST}(r) + \frac{1}{2} \left(p_r^2 \hat{V}_{p^2}^{ST}(r) + \hat{V}_{p^2}^{ST}(r) p_r^2 \right) + \hat{V}_{l^2}^{ST}(r) \mathbf{l}^2$$

one-body kinetic energy

central potentials

$$+ \sum_T \hat{V}_{ls}^T(r) \mathbf{l} \cdot \mathbf{s} + \hat{V}_{l^2ls}^T(r) \mathbf{l}^2 \mathbf{l} \cdot \mathbf{s}$$

spin-orbit potentials

$$+ \sum_T \hat{V}_t^T(r) \mathcal{S}_{12}(\mathbf{r}, \mathbf{r}) + \hat{V}_{trp_\Omega}^T(r) p_r \mathcal{S}_{12}(\mathbf{r}, \mathbf{p}_\Omega) + \hat{V}_{tll}^T(r) \mathcal{S}_{12}(\mathbf{l}, \mathbf{l}) +$$

$$\hat{V}_{tp_\Omega p_\Omega}^T(r) \mathcal{S}_{12}(\mathbf{p}_\Omega, \mathbf{p}_\Omega) + \hat{V}_{l^2tp_\Omega p_\Omega}^T(r) \mathbf{l}^2 \mathcal{S}_{12}(\mathbf{p}_\Omega, \mathbf{p}_\Omega)$$

tensor potentials

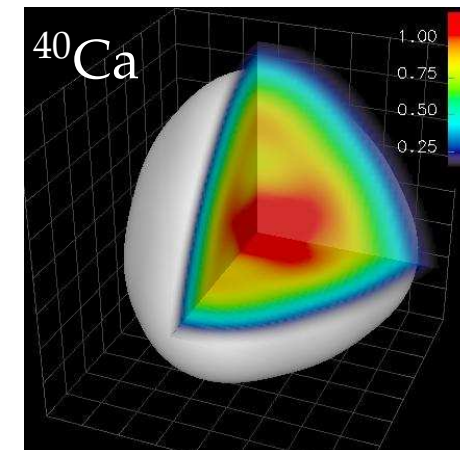
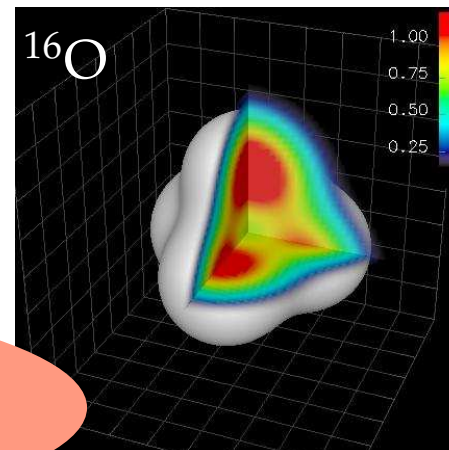
bulk of tensor force mapped onto central part of correlated interaction

tensor correlations also change the spin-orbit part of the interaction

Phenomenological Correction to V_{UCOM}

Effective two-body interaction

- FMD model space can't describe correlations induced by residual medium-long ranged tensor forces
 - use **longer ranged tensor correlator** to partly account for that
 - add phenomenological two-body correction term with a **momentum-dependend** central and (isospin-dependend) **spin-orbit** part
 - fit correction term to binding energies and radii of “closed-shell” nuclei (^4He , ^{16}O , ^{40}Ca), (^{24}O , ^{34}Si , ^{48}Ca)
- ➔ develop a new correction term that is checked against (small scale) No-Core Shell Model calculations



projected tetrahedral configurations are about 6 MeV lower in energy than “closed-shell” configurations

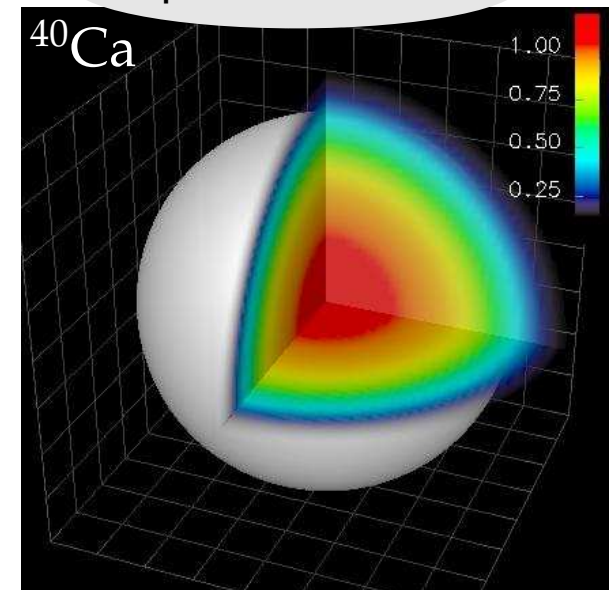
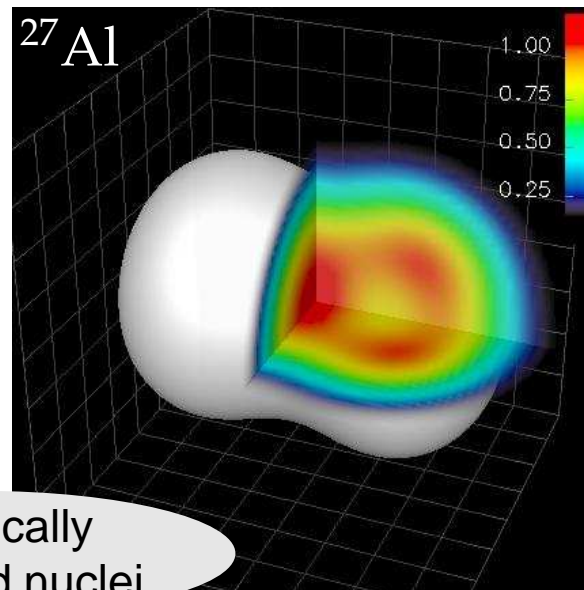
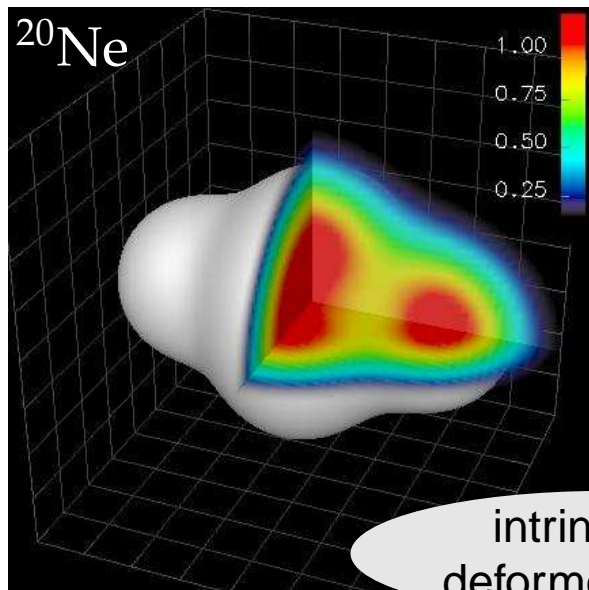
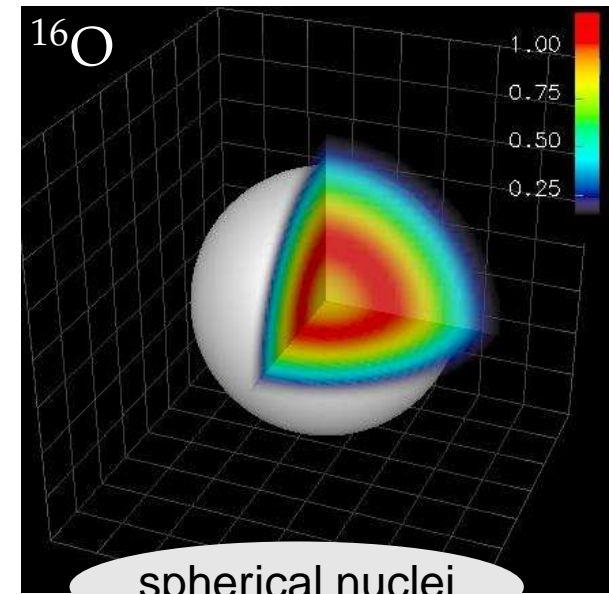
Perform Variation

Minimization

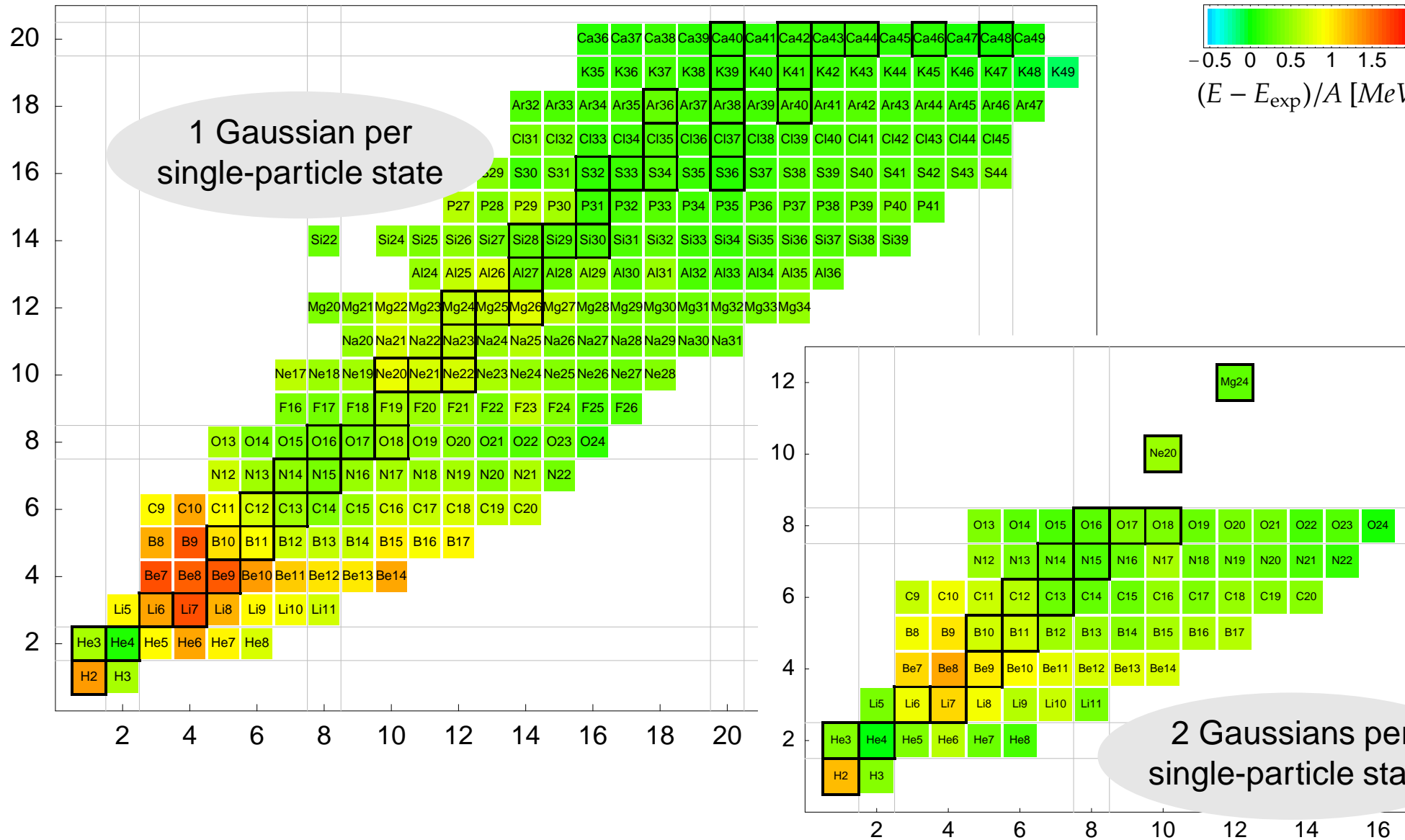
- minimize Hamiltonian with respect to all single-particle parameters q_k

$$\min_{\{q_k\}} \frac{\langle Q | \hat{H} - T_{cm} | Q \rangle}{\langle Q | Q \rangle}$$

- this is a Hartree-Fock calculation in our particular single-particle basis
- mean-field may break the symmetries of the Hamiltonian



$\rho^{(1)}(\mathbf{r}) [\rho_0]$



Beyond Mean-Field

Projection After Variation (PAV)

- mean-field may break symmetries of Hamiltonian
- restore inversion, translational and rotational symmetry by projection on parity, linear and angular momentum

$$\tilde{P}^{\mathbf{P}} = \frac{1}{(2\pi)^3} \int d^3X \exp\{-i(\tilde{\mathbf{P}} - \mathbf{P}) \cdot \mathbf{X}\}$$

$$\tilde{P}_{MK}^J = \frac{2J+1}{8\pi^2} \int d^3\Omega D_{MK}^J \star(\Omega) \tilde{R}(\Omega)$$

Variation After Projection (VAP)

- effect of projection can be large
- perform Variation after Parity Projection VAP $^{\pi}$
- perform VAP in GCM sense by applying **constraints** on **radius**, **dipole moment**, **quadrupole moment** or **octupole moment** and minimize the energy in the projected energy surface

➔ “real” VAP is possible for *p*-shell nuclei

Multiconfiguration Calculations

- **diagonalize** Hamiltonian in a set of projected intrinsic states

$$\left\{ |Q^{(a)}\rangle, \quad a = 1, \dots, N \right\}$$

$$\sum_{K'b} \langle Q^{(a)} | \tilde{H} \tilde{P}_{KK'}^{J\pi} \tilde{P}^{\mathbf{P}=0} | Q^{(b)} \rangle \cdot c_{K'b}^{(i)} = E^{J\pi(i)} \sum_{K'b} \langle Q^{(a)} | \tilde{P}_{KK'}^{J\pi} \tilde{P}^{\mathbf{P}=0} | Q^{(b)} \rangle \cdot c_{K'b}^{(i)}$$

Angular Momentum Projection

Intrinsic State

- the intrinsic state is in general not an angular momentum eigenstate
- it is a superposition of angular momentum eigenstates

$$|Q\rangle = \sum_{JM\alpha} |Q; JM\alpha\rangle c_{JM\alpha}, \quad \mathbf{J}^2 |Q; JM\alpha\rangle = J(J+1) |Q; JM\alpha\rangle, \quad J_z |Q; JM\alpha\rangle = M |Q; JM\alpha\rangle$$

Angular Momentum Projection Operator

$$P_{\tilde{M}K}^J = \frac{2J+1}{8\pi^2} \int d^3\Omega D_{MK}^J(\Omega) R(\Omega)$$

- Rotation Operator $R(\Omega)$ rotates the wave function with the Euler angles $\Omega = (\alpha, \beta, \gamma)$
- Wigner D -matrix

$$D_{MK}^J(\Omega) = \langle JM | R(\Omega) | JK \rangle = \langle JM | e^{iJ_z\alpha} e^{iJ_y\beta} e^{iJ_z\gamma} | JK \rangle = \exp\{-iM\alpha\} d_{MK}^J(\beta) \exp\{iM\gamma\}$$

- not a true projection operator

$$(P_{\tilde{M}K}^J)^\dagger P_{\tilde{M}'K'}^{J'} = \delta_{JJ'} \delta_{M,M'} P_{\tilde{K}K'}^J$$

Angular Momentum Projection

K-mixing

- angular momentum eigenstates are linear combinations of projected states with different K

$$|Q; JM\alpha\rangle = \sum_K P_{\sim MK}^J |Q\rangle c_K^{J\alpha}$$

- solve the generalized eigenvalue problem to get the eigenstates

$$\sum_{K'} \langle Q | (P_{\sim MK}^J)^\dagger H P_{\sim MK'}^J | Q \rangle c_{K'}^{J\alpha} = E^{J\alpha} \sum_{K'} \langle Q | (P_{\sim MK}^J)^\dagger P_{\sim MK'}^J | Q \rangle c_{K'}^{J\alpha}$$

- as the Hamiltonian commutes with rotations this simplifies to

$$\sum_{K'} \langle Q | H P_{\sim KK'}^J | Q \rangle c_{K'}^{J\alpha} = E^{J\alpha} \sum_{K'} \langle Q | P_{\sim KK'}^J | Q \rangle c_{K'}^{J\alpha}$$

Axial Symmetry

- if $|Q\rangle$ is an eigenstate of J_z the integrations over α and γ become trivial and only the β integration remains

Center-Of-Mass Problem

- Hamiltonian does not couple internal and center-of-mass motion

$$\tilde{H} = \tilde{H}_{\text{internal}} + \tilde{T}_{\text{cm}}$$

- in product states (Slater determinants) the internal motion is entangled with the center-of-mass motion
- ➔ zero-th order correction: always use internal operators $\tilde{H}_{\text{internal}} = \tilde{H} - \tilde{T}_{\text{cm}}, \dots$
- ➔ in the special case where all widths a are equal the wave function factorizes in the internal wave function and the center-of-mass wave function

$$\langle \mathbf{x}_1, \dots, \mathbf{x}_A | Q \rangle = \Phi_{\text{internal}}(\xi_1, \dots, \xi_A) \Phi_{\text{cm}}^a(\mathbf{X})$$

with coordinates $\xi_i = \mathbf{x}_i - \mathbf{X}$ and $\mathbf{X} = \frac{1}{A} \sum_i \mathbf{x}_i$

- ➔ in the general case we project the wave function on total momentum $\mathbf{P} = 0$ with the projection operator

$$\tilde{P}^{\mathbf{P}} = \frac{1}{(2\pi)^3} \int d^3X \exp\{-i(\tilde{\mathbf{P}} - \mathbf{P}) \cdot \mathbf{X}\}$$

The projected wave function is then given as

$$\langle \mathbf{x}_1, \dots, \mathbf{x}_A | \tilde{P}^{\mathbf{P}} | Q \rangle = \frac{1}{(2\pi)^3} \int d^3X e^{i\mathbf{P} \cdot \mathbf{X}} \langle \mathbf{x}_1 - \mathbf{X}, \dots, \mathbf{x}_A - \mathbf{X} | Q \rangle$$

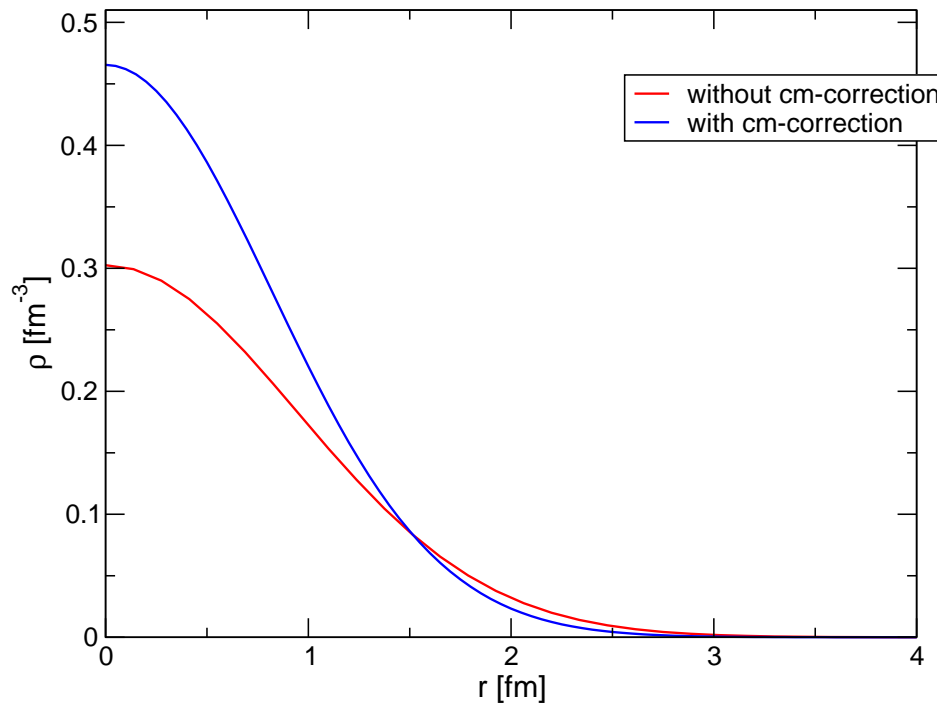
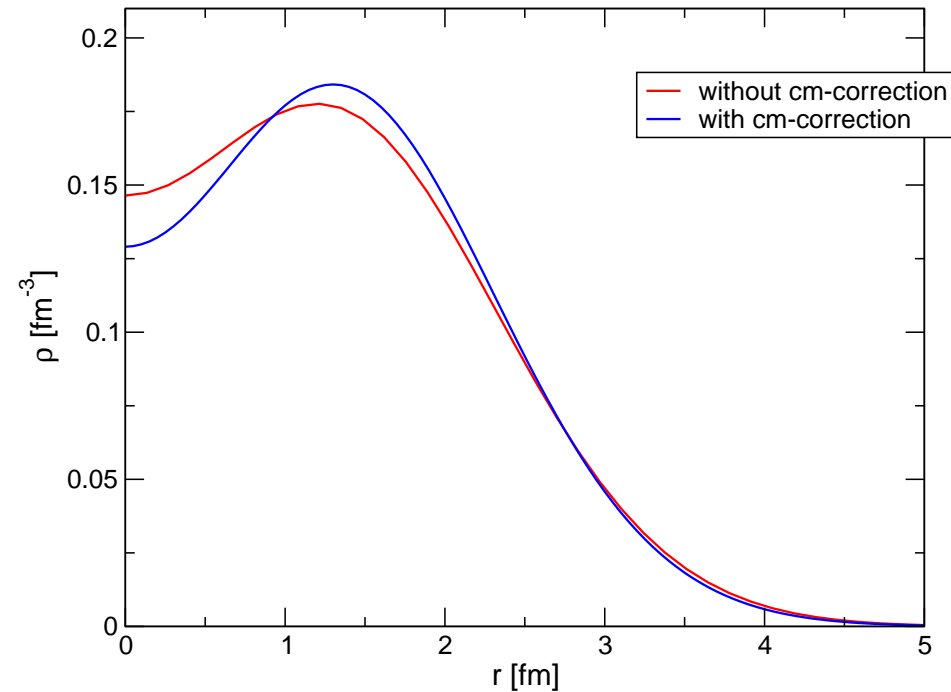
Center-Of-Mass Problem

- one-body density calculated with Slater determinant

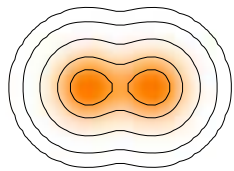
$$\rho^{(1)}(\mathbf{r}) = \langle \Psi | \sum_i \delta(\mathbf{r}_i - \mathbf{r}) | \Psi \rangle$$

- density of internal wave function

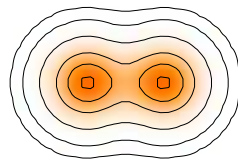
$$\rho_{\text{internal}}^{(1)}(\mathbf{r}) = \langle \Psi | \sum_i \delta(\mathbf{r}_i - \mathbf{R} - \mathbf{r}) | \Psi \rangle$$

 ${}^4\text{He}$  ${}^{16}\text{O}$ 

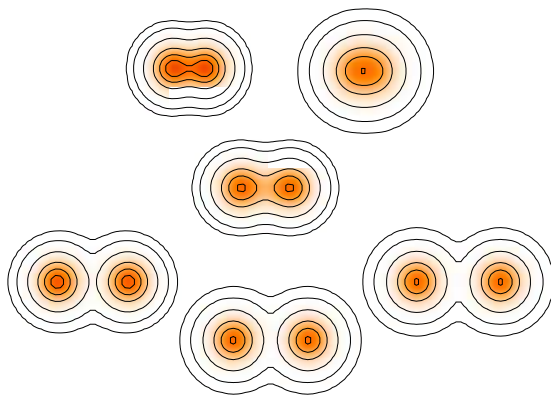
V/PAV



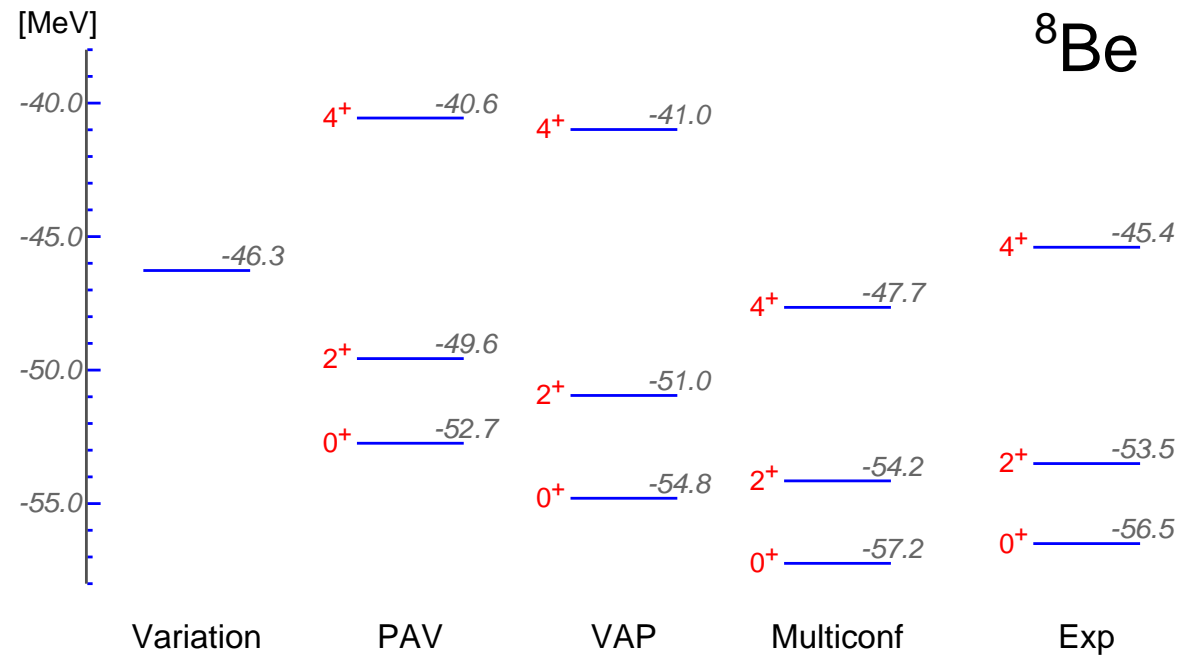
VAP



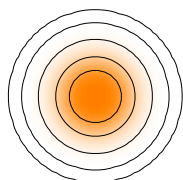
Multiconfig



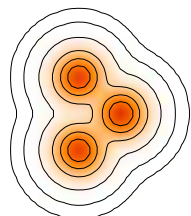
	E_b [MeV]	r_{charge} [fm]	$B(E2)$ [$e^2\text{fm}^4$]
PAV	52.7	2.39	9.31
VAP	54.8	2.49	15.36
Multiconfig	57.2	2.74	30.39
Exp	56.5		



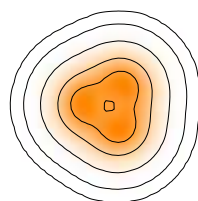
V/PAV



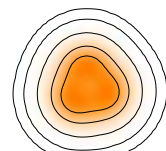
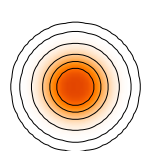
VAP α



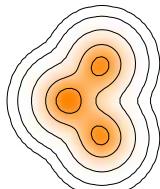
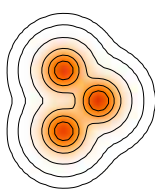
V^π /PAV $^\pi$



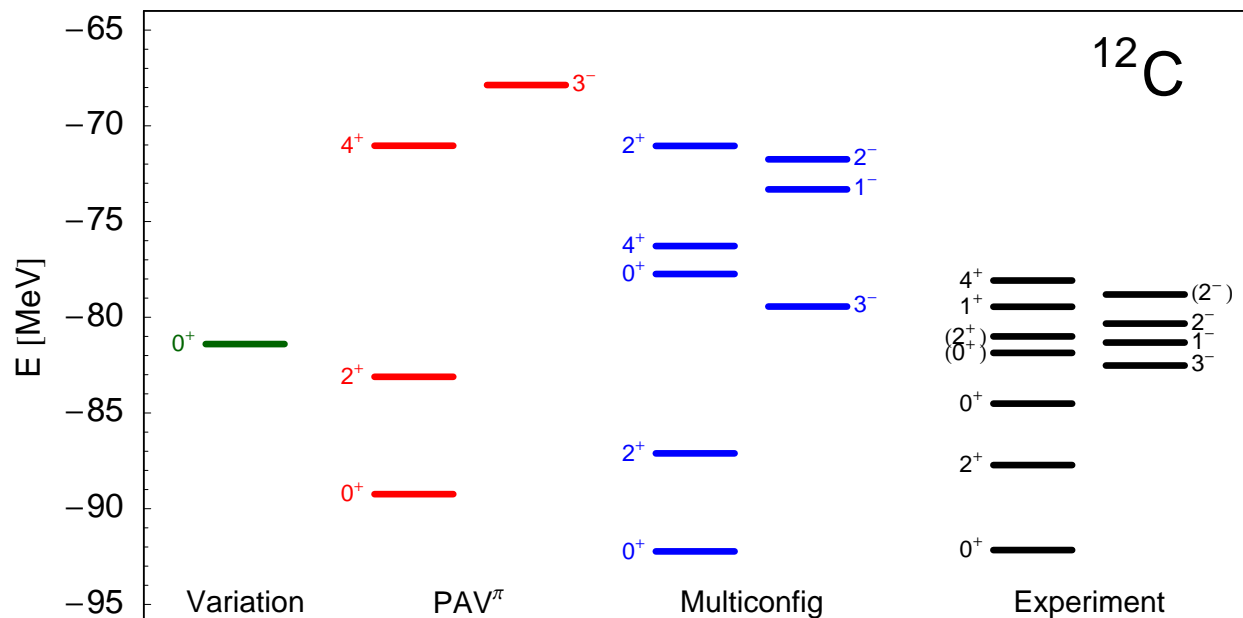
Multiconfig



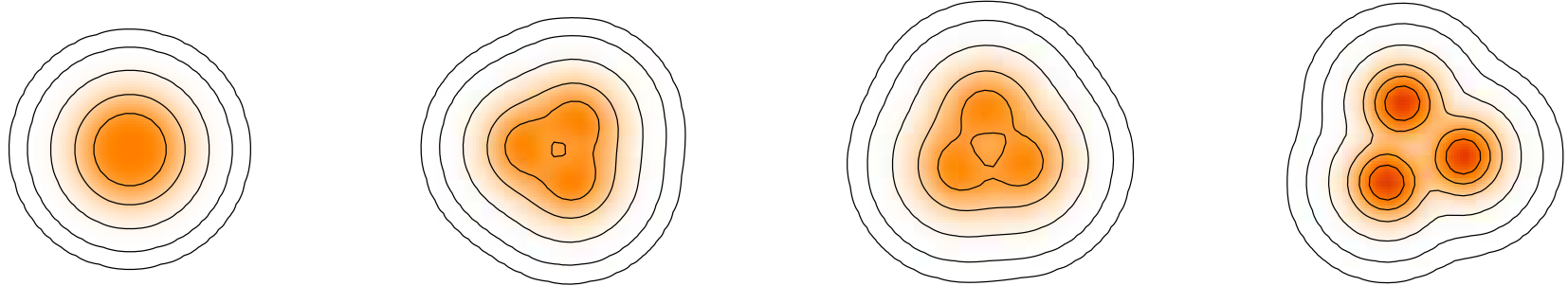
VAP



	E_b [MeV]	r_{charge} [fm]	$B(E2)$ [$e^2\text{fm}^4$]
V/PAV	81.4	2.36	-
VAP α -cluster	79.1	2.70	76.9
PAV $^\pi$	88.5	2.51	36.3
VAP	89.2	2.42	26.8
Multiconfig	92.2	2.52	42.8
Experiment	92.2	2.47	39.7 ± 3.3



Shell-structure versus Cluster states in ^{12}C



	intrinsic		projected		intrinsic		projected		intrinsic		projected	
$\langle \tilde{H} \rangle$	-81.4	-81.5	-77.0	-88.5	-74.1	-85.5	-57.0	-75.9	-57.0	-75.9	-57.0	-75.9
$\langle \tilde{T} \rangle$	212.1	212.1	189.2	186.1	182.8	179.0	213.9	201.4	213.9	201.4	213.9	201.4
$\langle \tilde{V}_{ls} \rangle$	-39.8	-40.2	-12.0	-17.1	-5.8	-8.0	-	-	-	-	-	-
$\sqrt{\langle \tilde{r}^2 \rangle}$	2.22	2.22	2.40	2.37	2.45	2.42	2.44	2.42	2.44	2.44	2.42	2.42

spin-orbit force “breaks” clusters

cluster states strongly “feel” projection

Applications



Helium Isotopes

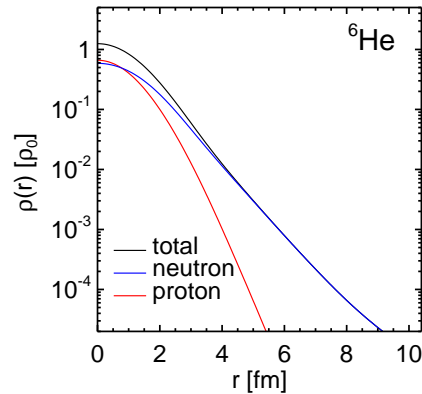
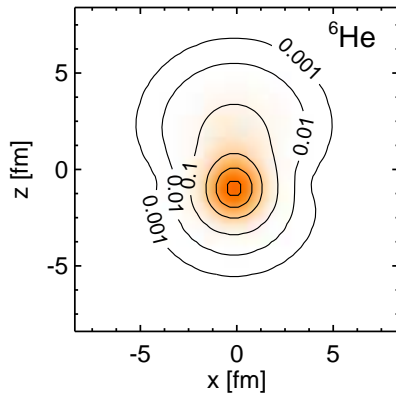
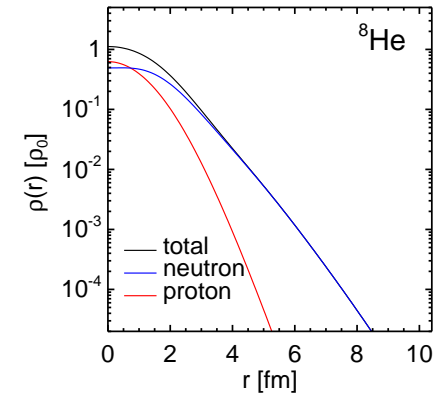
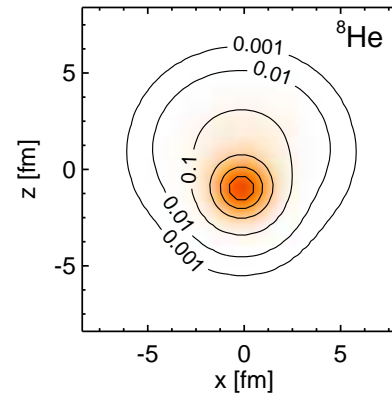
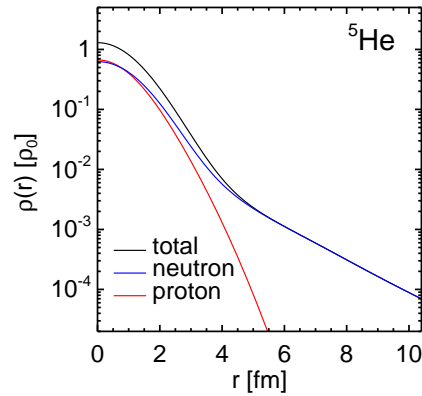
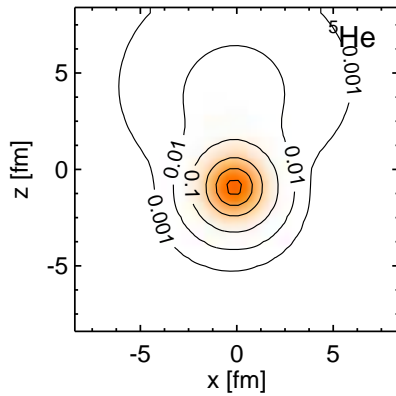
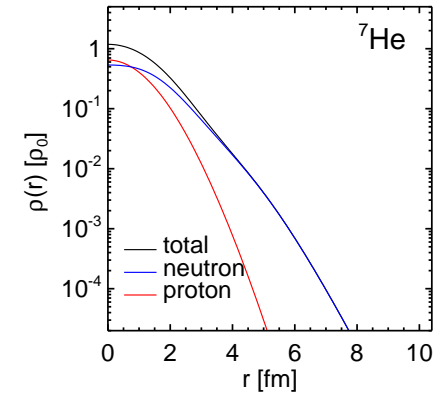
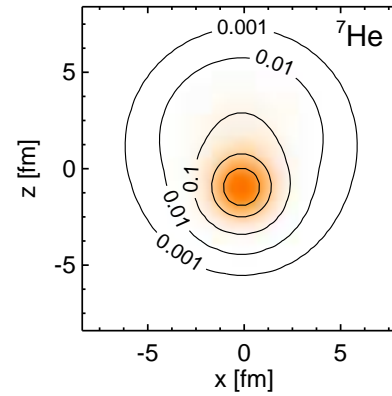
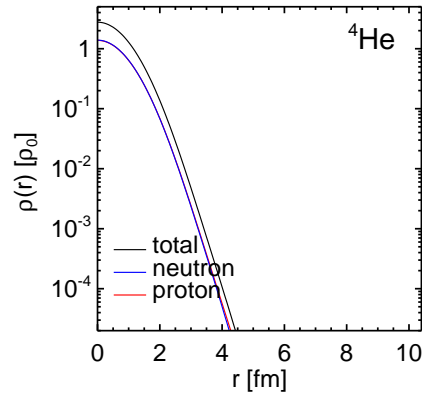
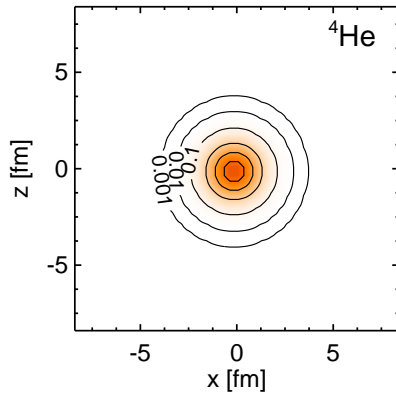
Lithium Isotopes

Beryllium Isotopes

Carbon Isotopes

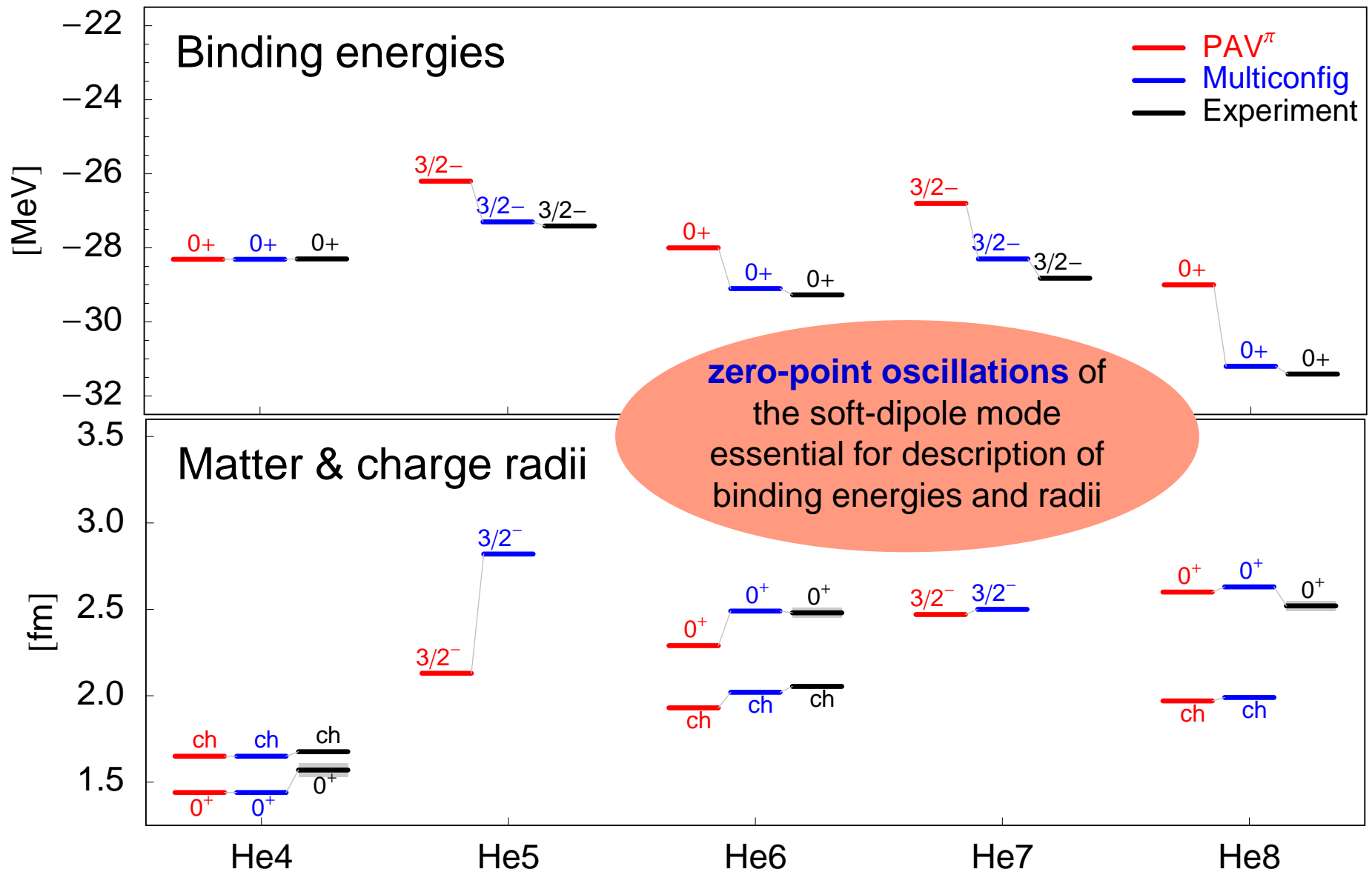
Applications Helium Isotopes

dipole and quadrupole constraints



- intrinsic nucleon densities of VAP states
- radial densities from multiconfiguration calculations

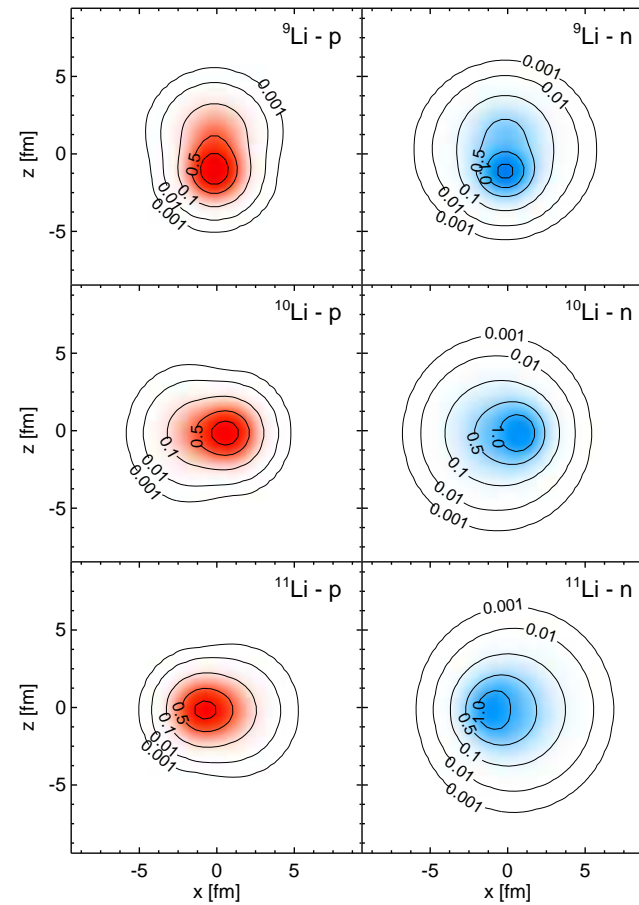
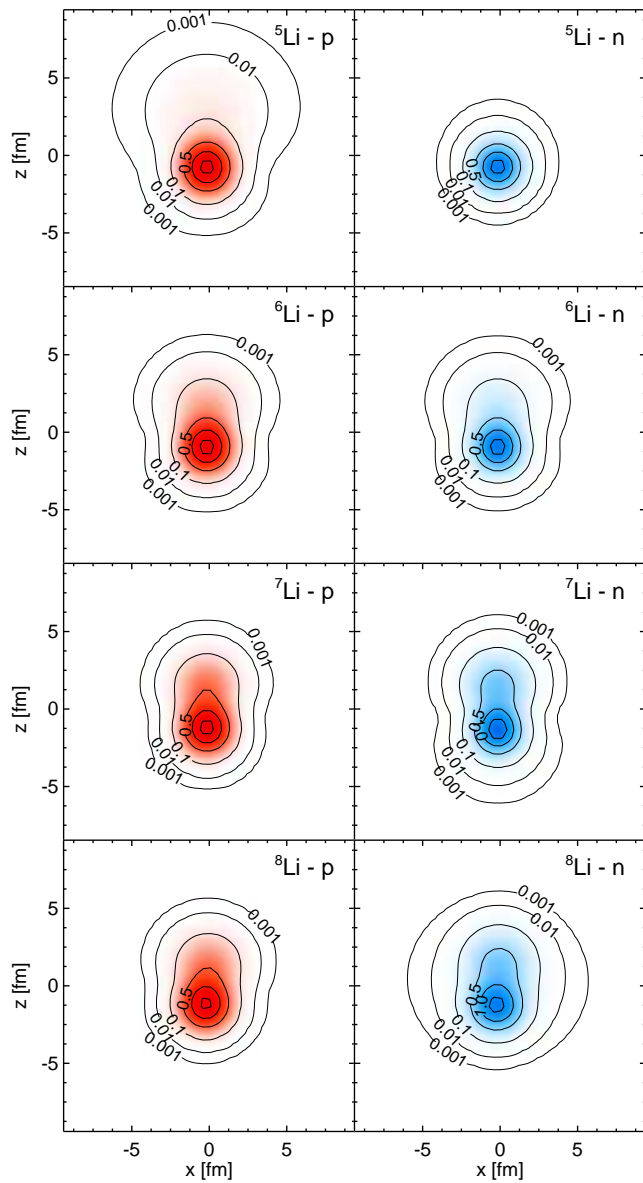
- Applications
- **Helium Isotopes**



^6He charge radius: L.-B. Wang et al, Phys. Rev. Lett. **94** (2004) 142501

Applications Lithium Isotopes

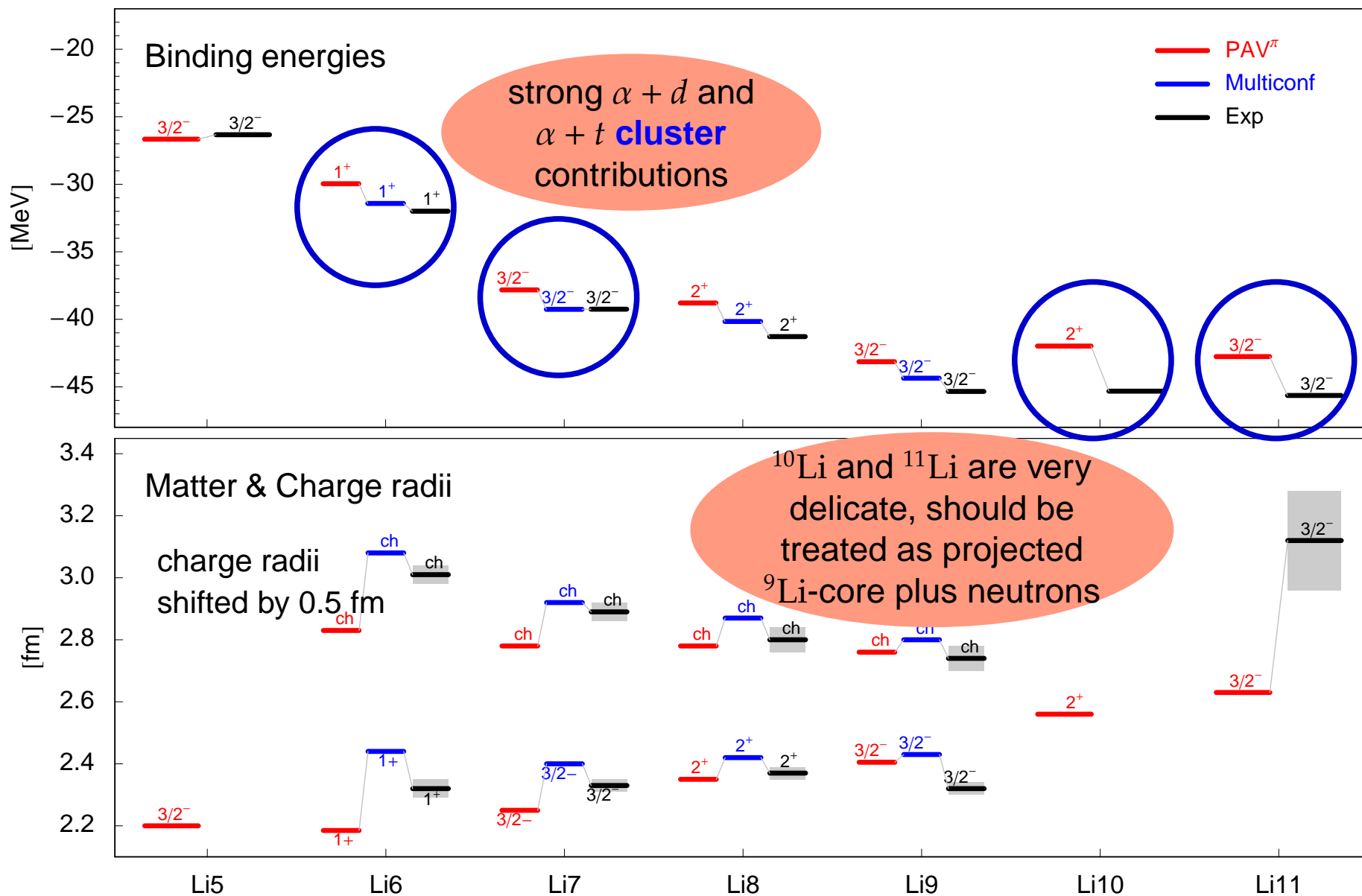
quadrupole constra



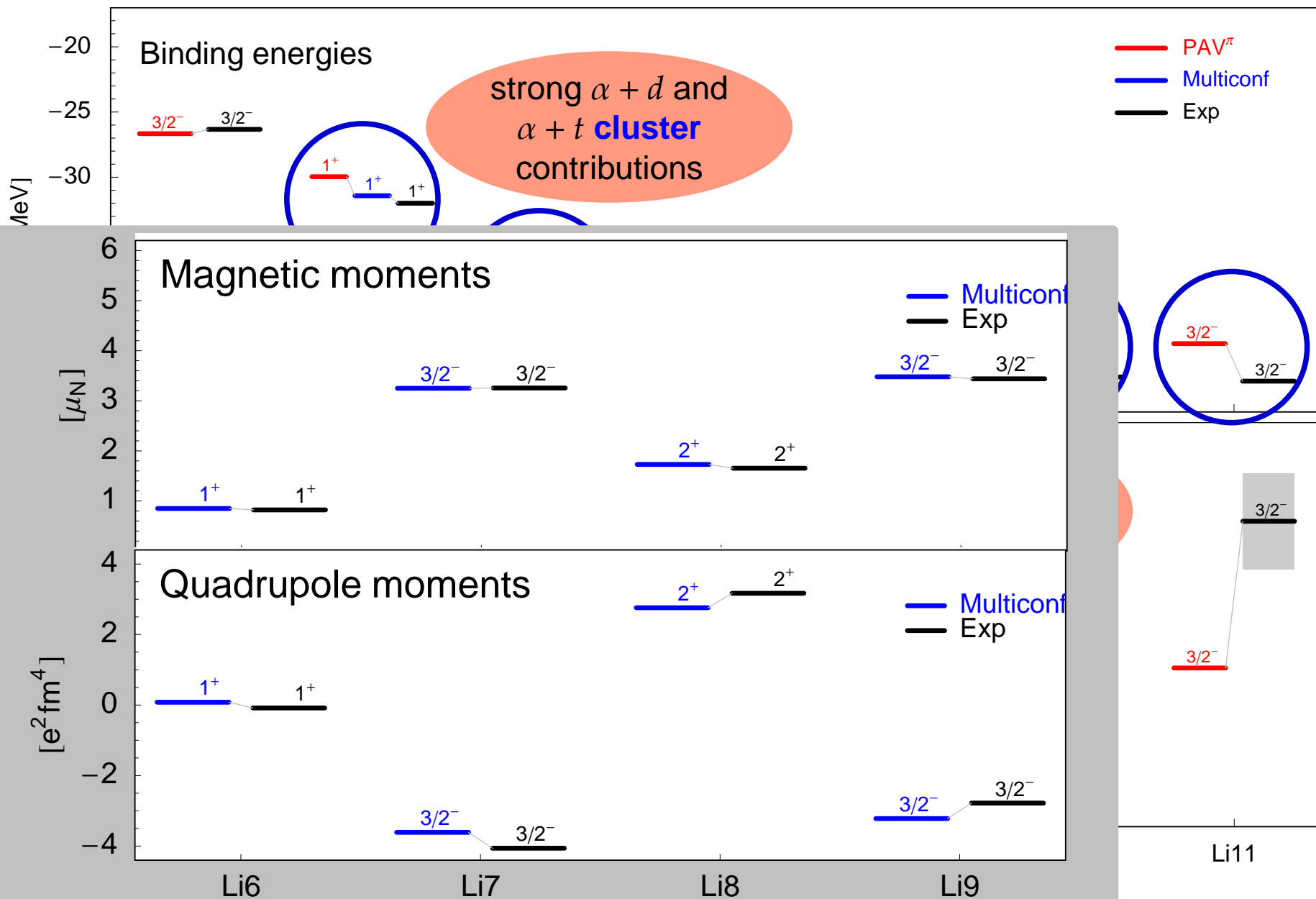
➔ intrinsic densities of V^π states

Applications Lithium Isotopes

with cm-project

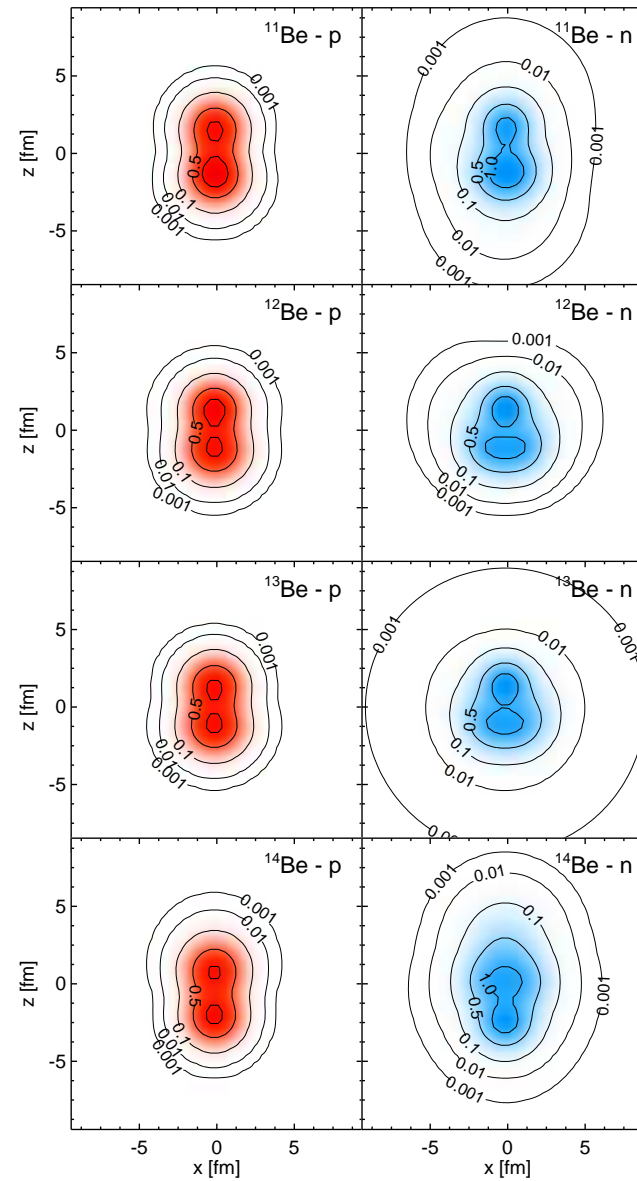
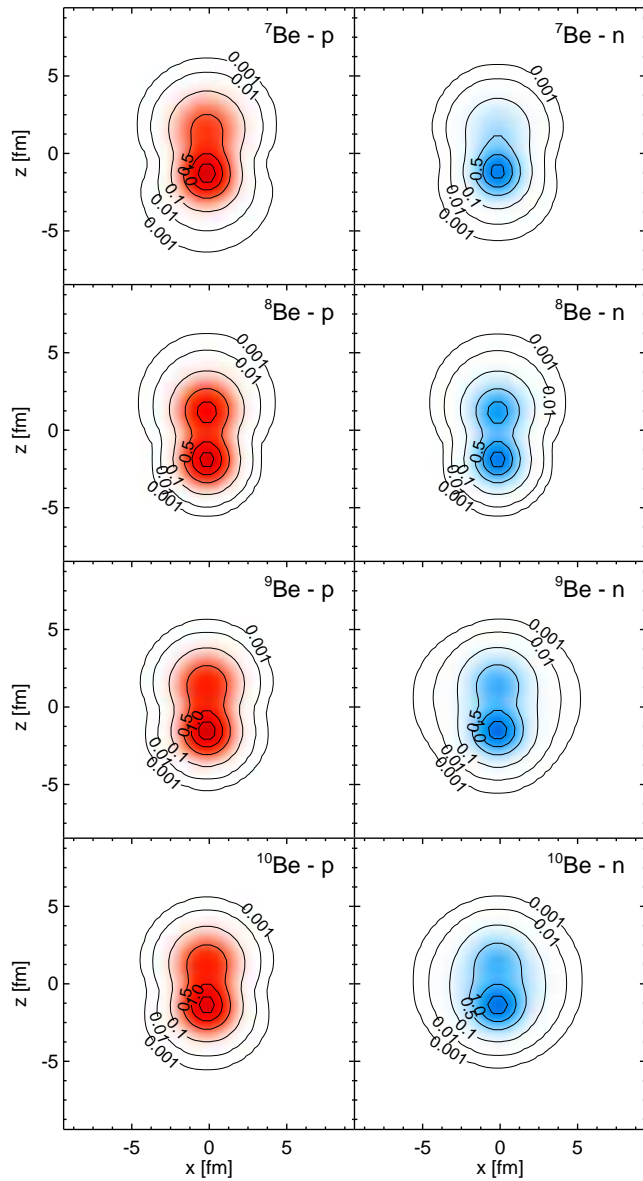


^{6-9}Li charge radii: G. Ewald et al, Phys. Rev. Lett. **93** (2004) 113002



⁶Li charge radii: G. Ewald et al, Phys. Rev. Lett. **93** (2004) 113002

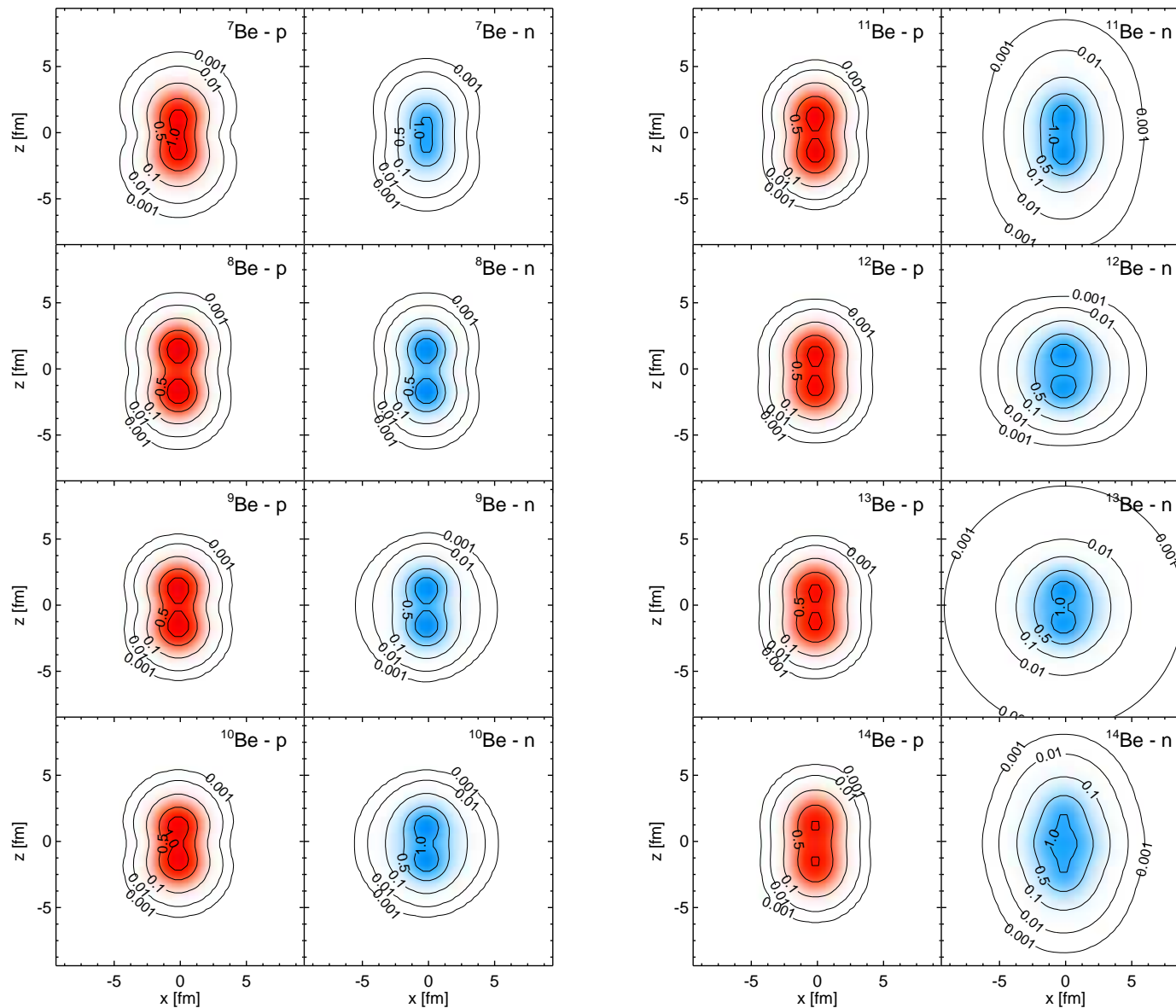
Beryllium Isotopes



→ intrinsic densities of V^π states

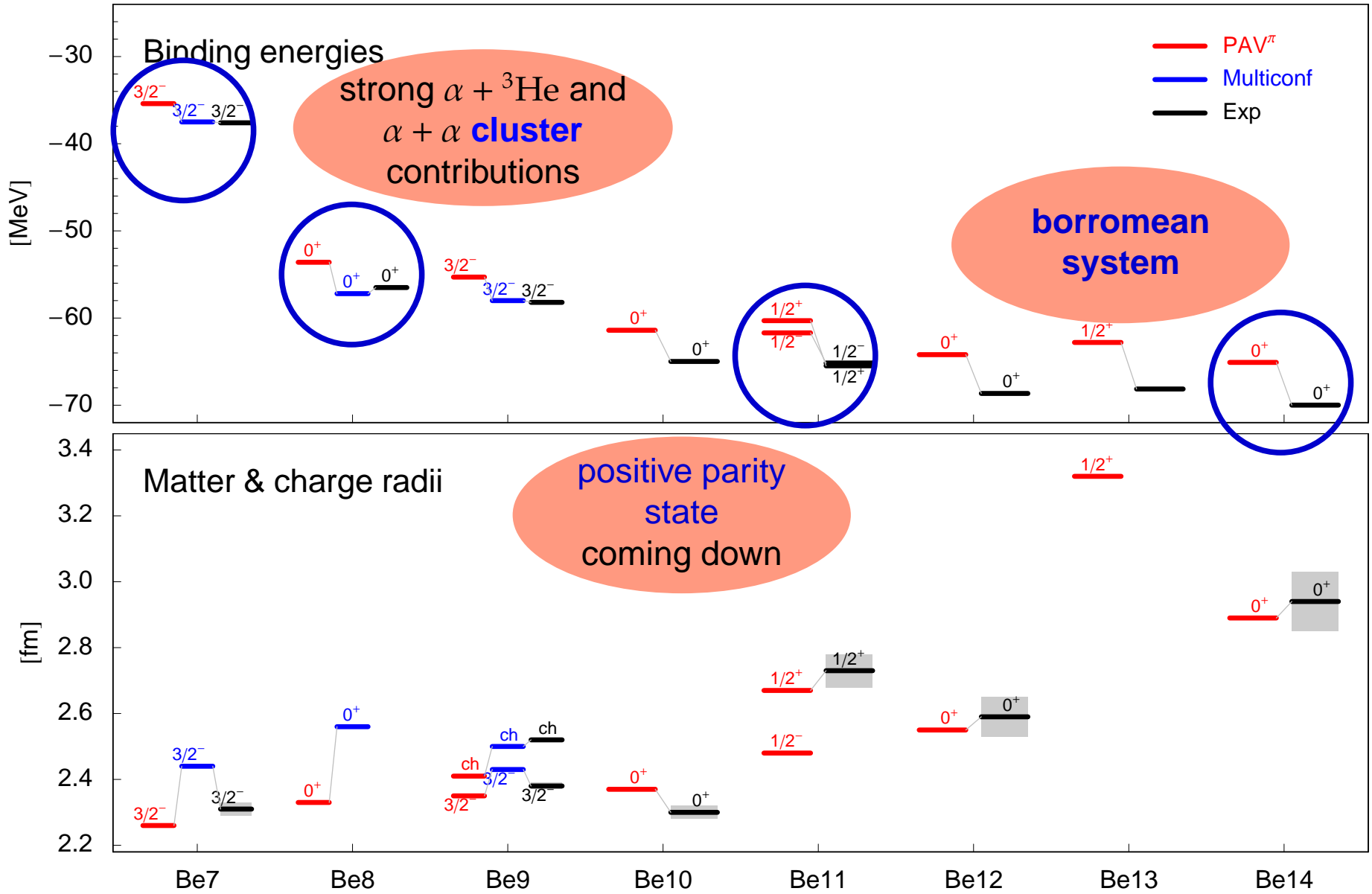
cluster structure evolves with addition of neutrons

Beryllium Isotopes



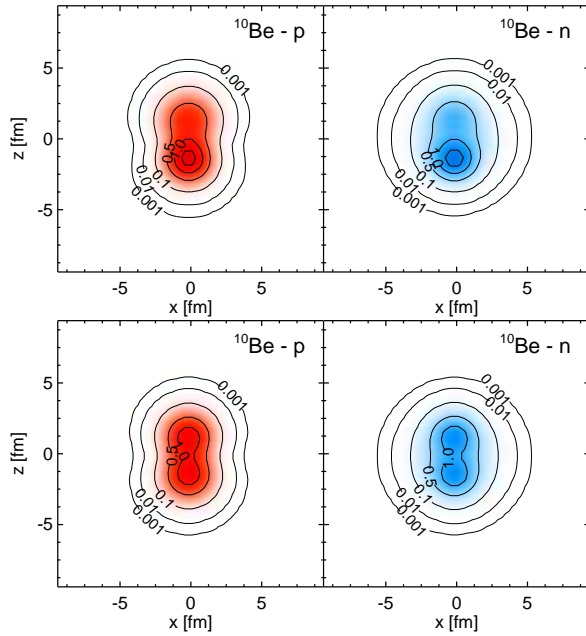
➔ intrinsic densities of parity projected V^π states

cluster structure evolves with addition of neutrons

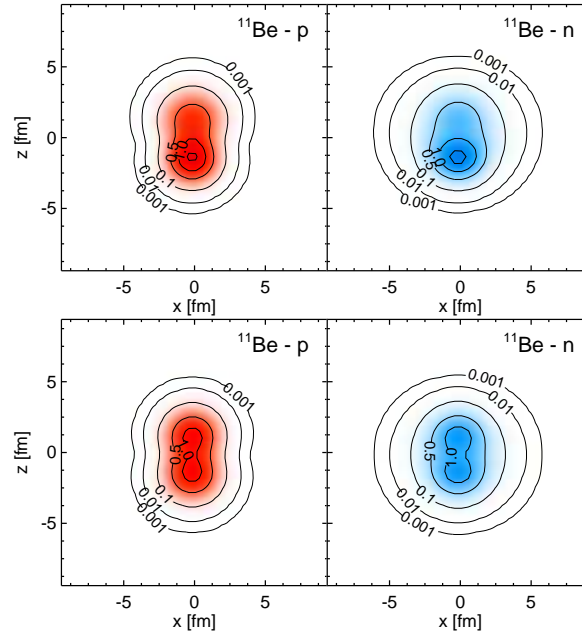


- Applications
- ^{11}Be positive parity intruder

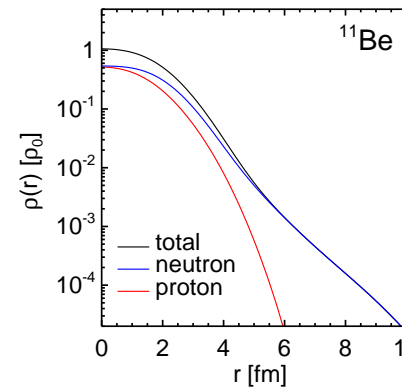
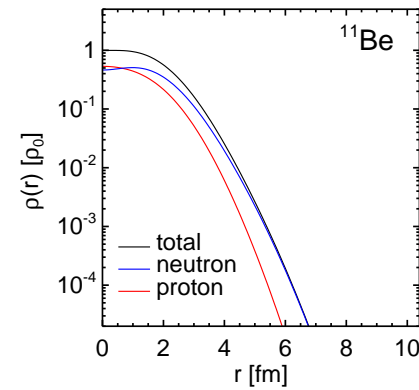
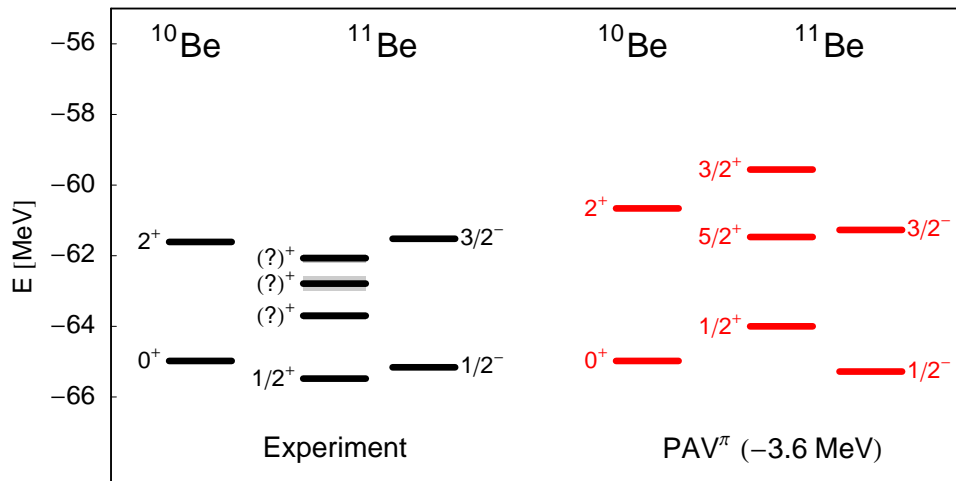
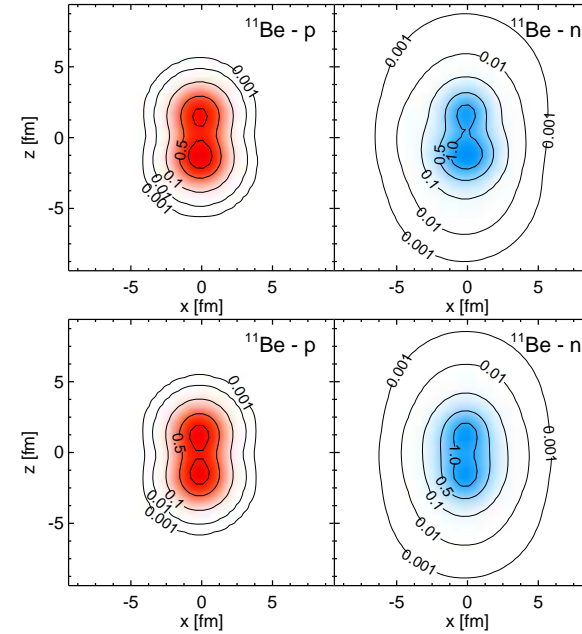
^{10}Be



^{11}Be negative parity



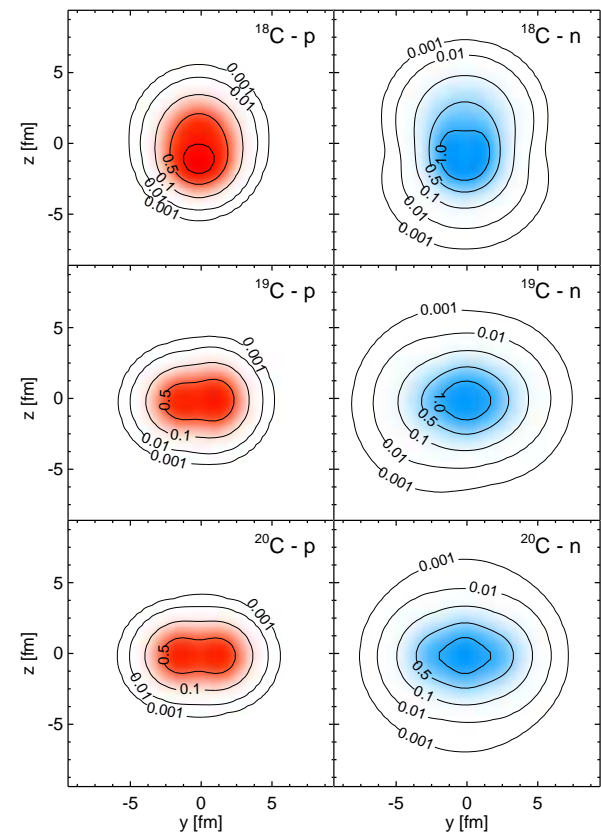
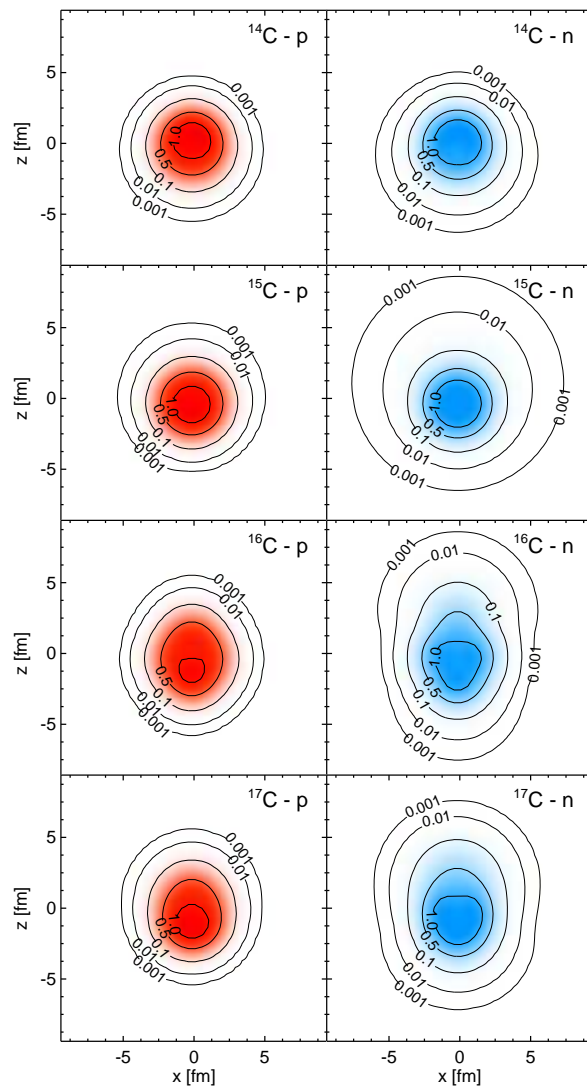
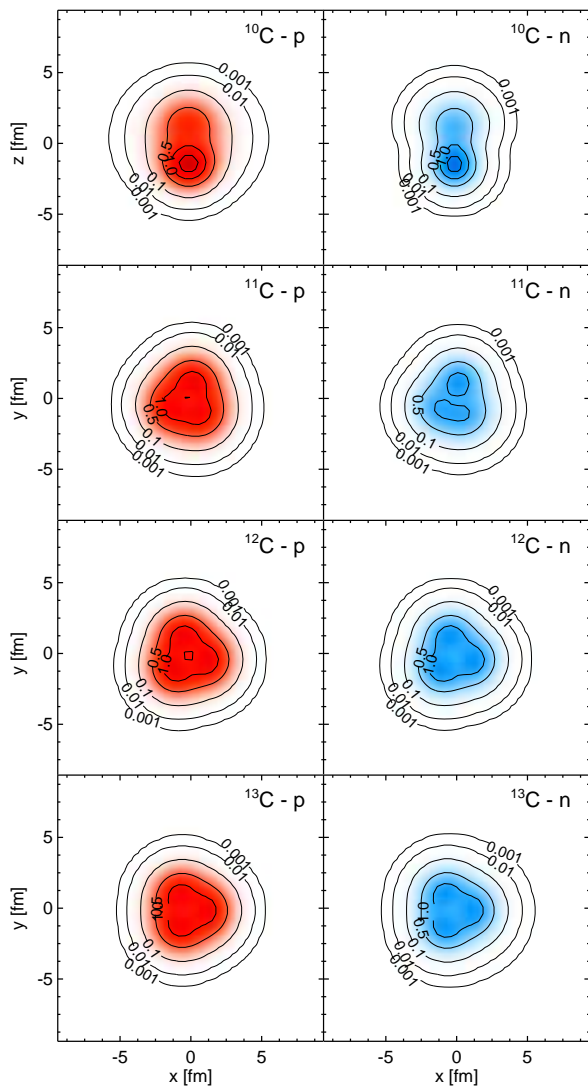
^{11}Be positive parity



➔ $1/2^+$ state has a neutron halo

Applications

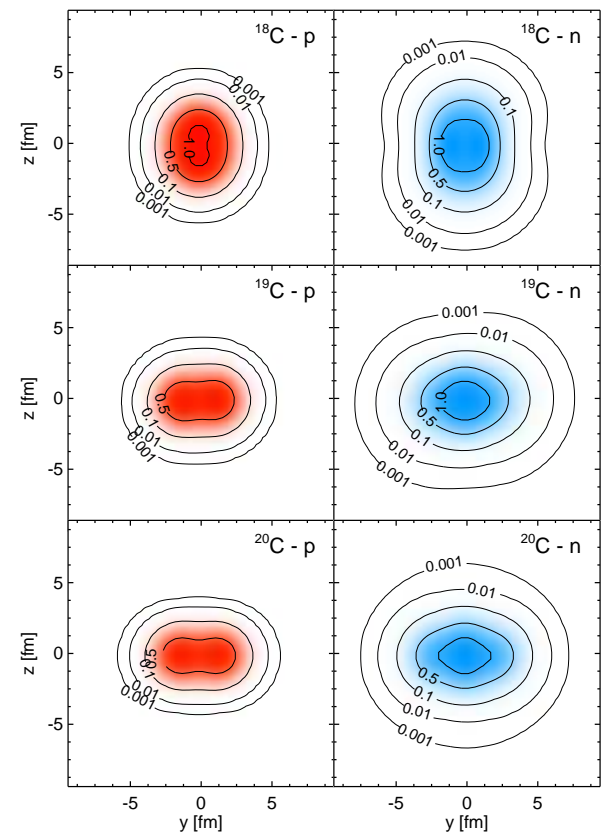
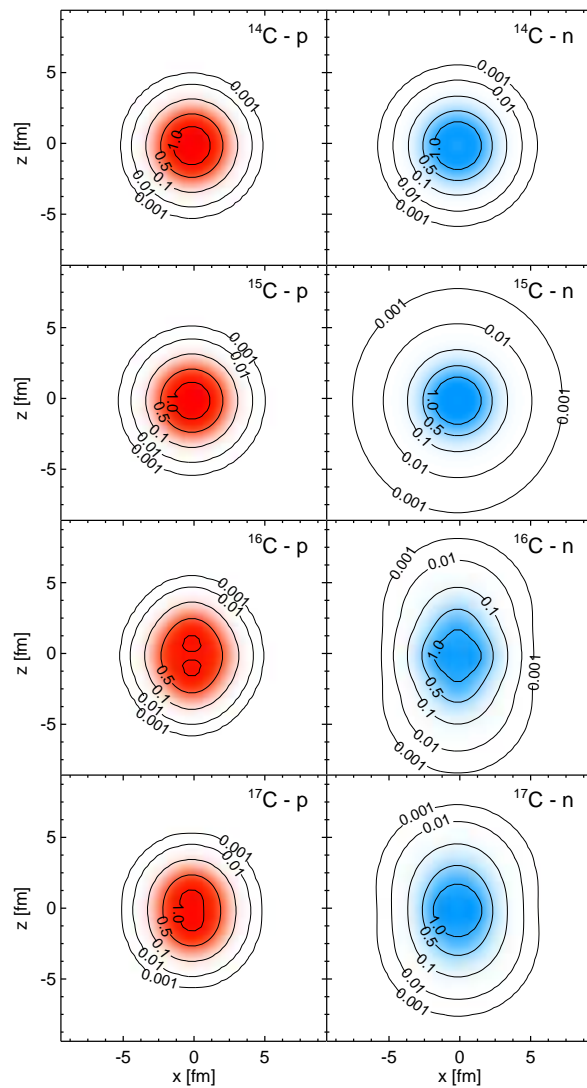
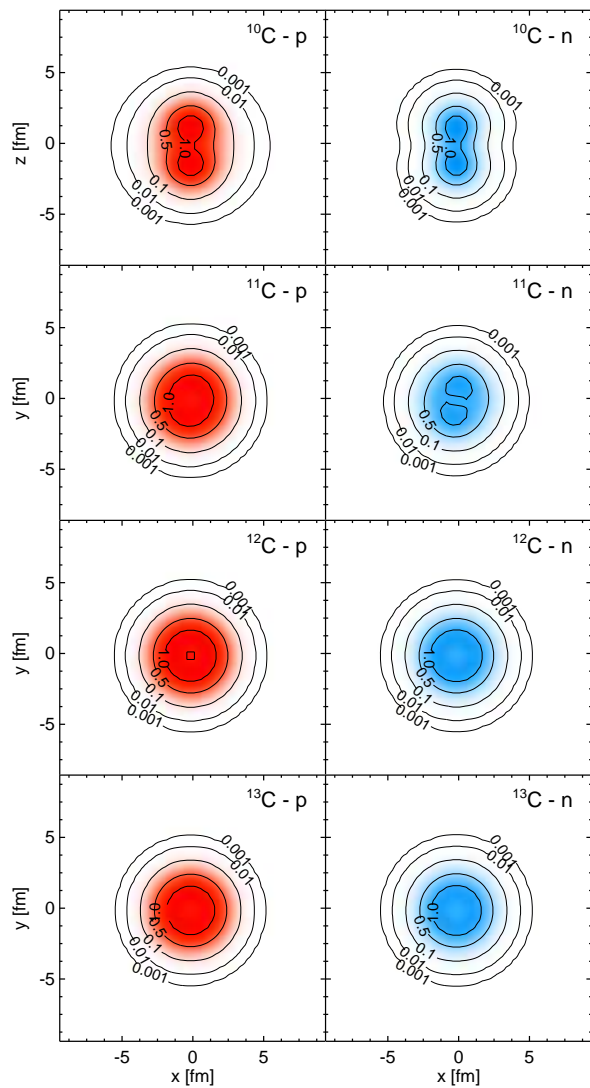
Carbon Isotopes



➔ intrinsic densities of V^π states

Applications

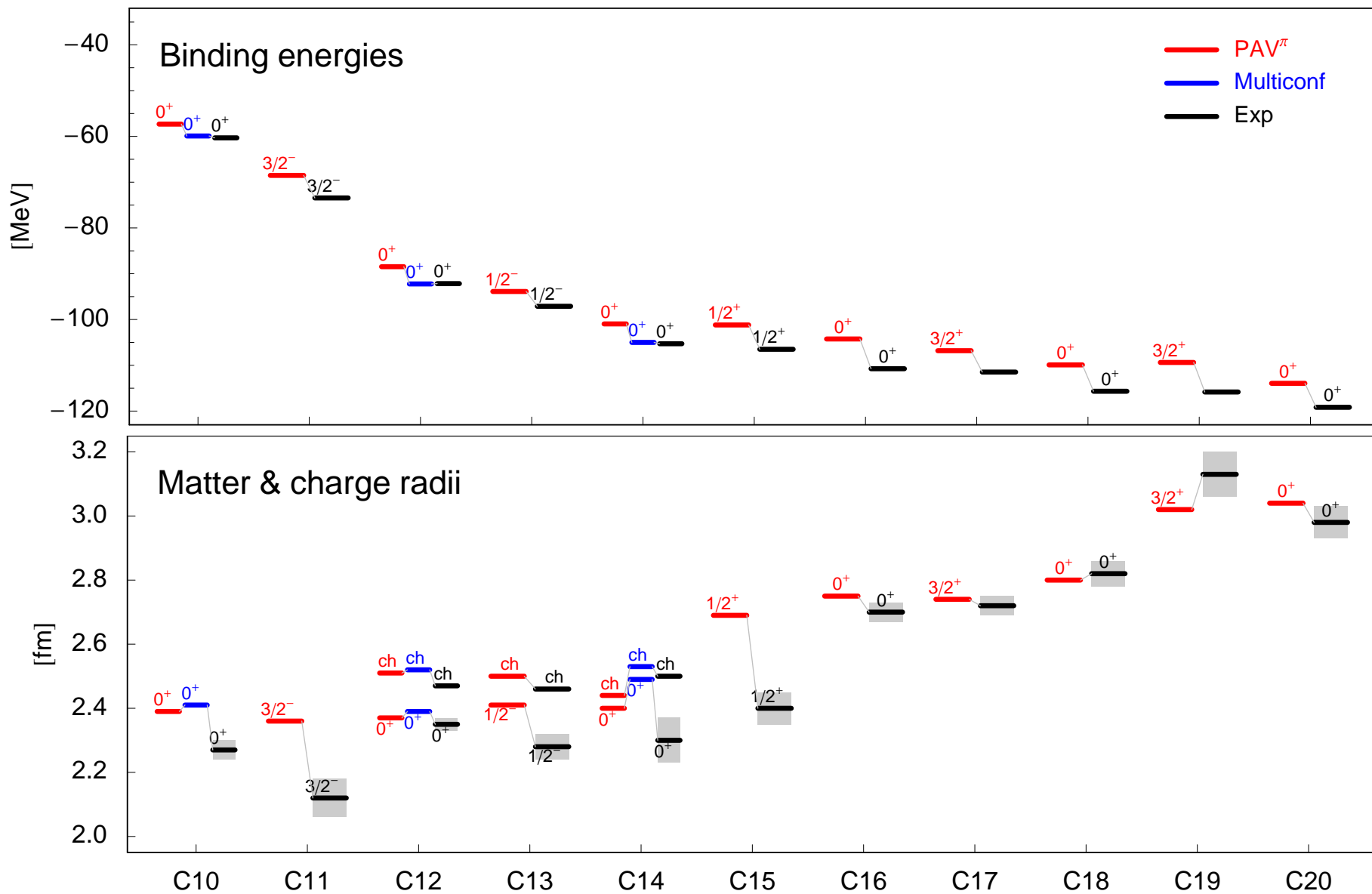
Carbon Isotopes



➔ intrinsic densities of parity projected V^π states

- Applications
- **Carbon Isotopes**

quadrupole constra



Hoyle State in ^{12}C



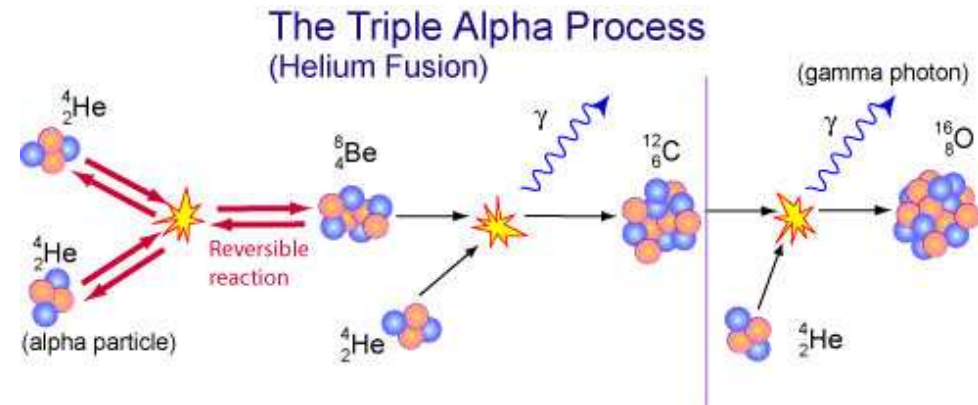
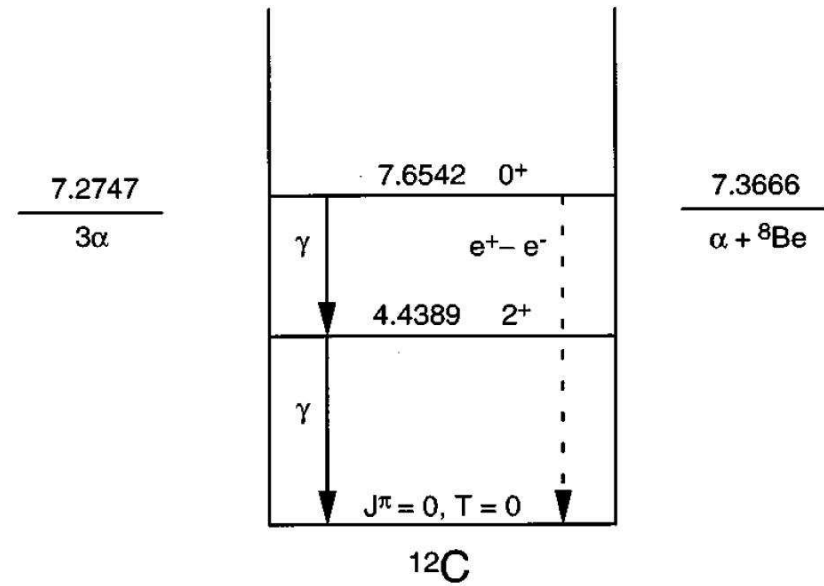
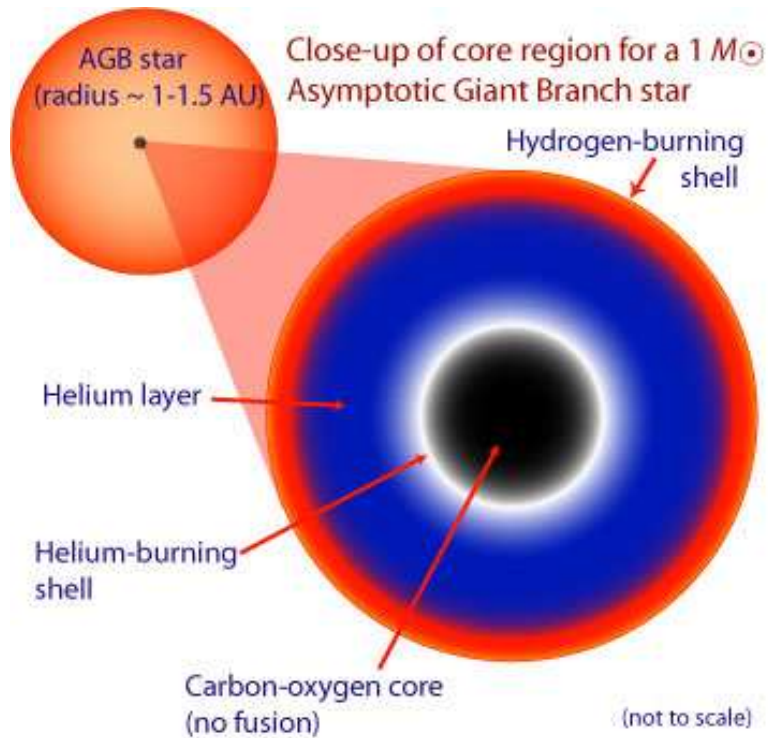
Astrophysical Motivation

Nuclear Structure

- What is the structure of the Hoyle state ?
- higher lying 0^+ and 2^+ states
- ➔ Compare to α -cluster model

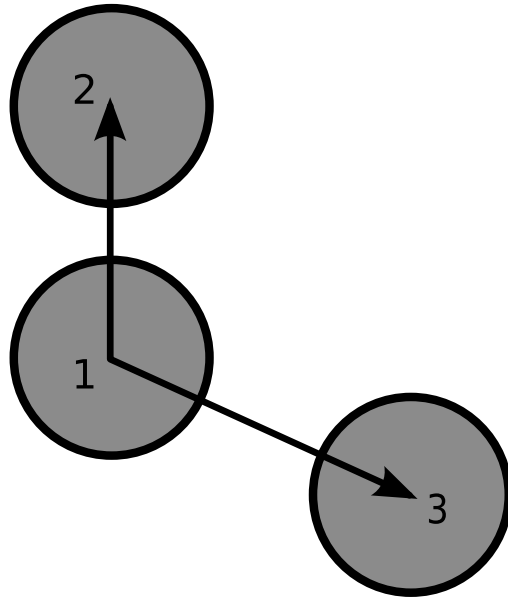
Phys. Rev. Lett. 98, 032501 (2007)

- Hoyle State
- Triple α Reaction



http://outreach.atnf.csiro.au/education/senior/astrophysics/stellarevolution_postmain.html

- Hoyle State
- **Microscopic α -Cluster Model**



$$R_{12} = (2, 4, \dots, 10) \text{ fm}$$

$$R_{13} = (2, 4, \dots, 10) \text{ fm}$$

$$\cos(\vartheta) = (1.0, 0.8, \dots, -1.0)$$

altogether 165 configurations

Basis States

- describe Hoyle State as a system of 3 ^4He nuclei

$$|\Psi_{3\alpha}(\mathbf{R}_1, \mathbf{R}_2, \mathbf{R}_3); JMK\pi\rangle = P_{MK}^J P^\pi \mathcal{A} \left\{ |\psi_\alpha(\mathbf{R}_1)\rangle \otimes |\psi_\alpha(\mathbf{R}_2)\rangle \otimes |\psi_\alpha(\mathbf{R}_3)\rangle \right\}$$

Volkov Interaction

- simple central interaction
- parameters adjusted to reproduce α binding energy and radius, $\alpha - \alpha$ scattering data and Hoyle State ground state energy
- ✗ only reasonable for ^4He , ^8Be and ^{12}C nuclei

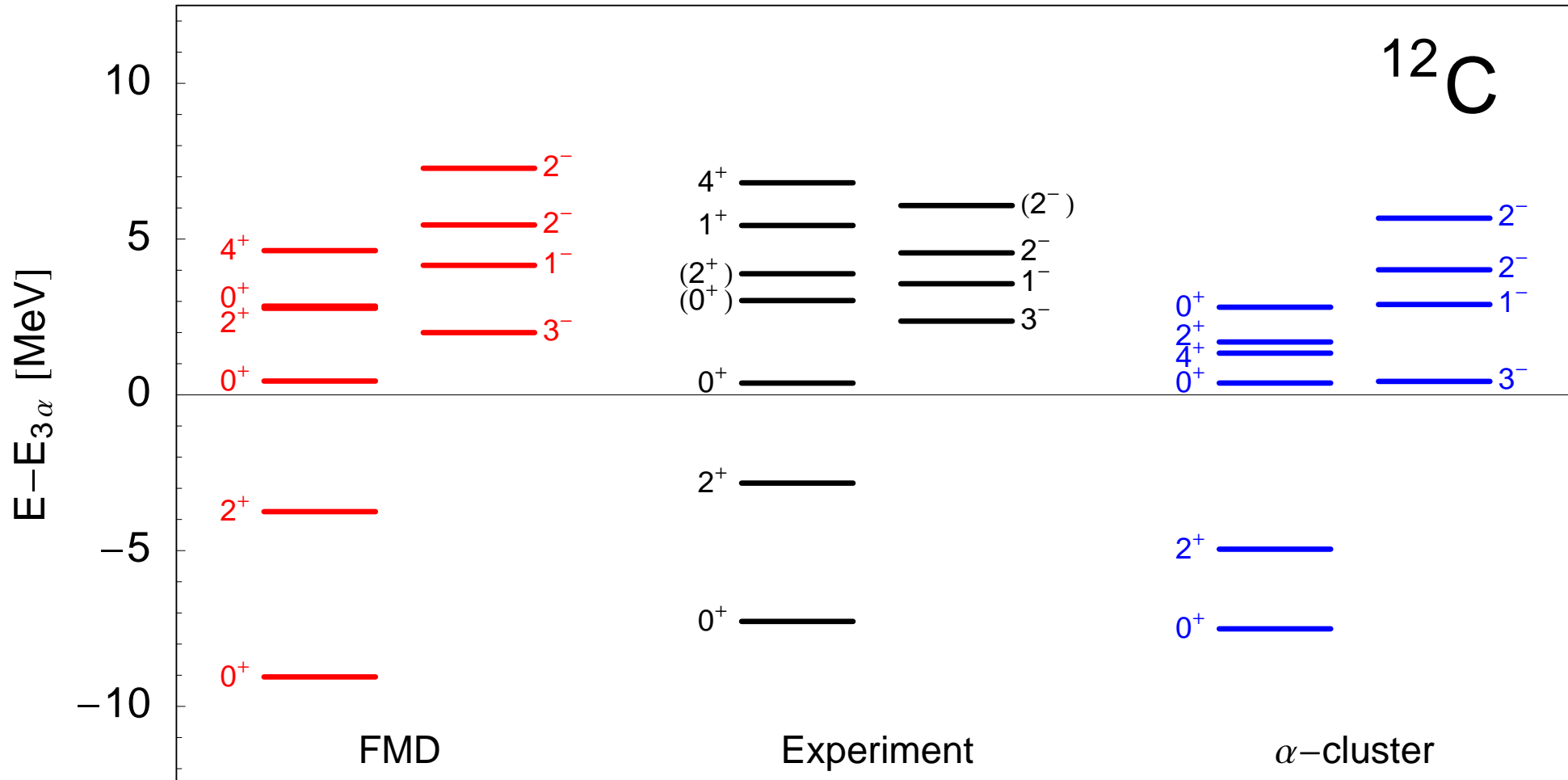
Basis States

- 20 FMD states obtained in Variation after Projection on 0^+ and 2^+ with constraints on the radius
 - 42 FMD states obtained in Variation after Projection on parity with constraints on radius and quadrupole deformation
 - 165 α -cluster configurations
- projected on angular momentum and linear momentum

Interaction

- FMD interaction based on UCOM interaction with phenomenological two-body correction term fitted to energies and radii of doubly-magic nuclei
- not explicitly tuned for α - α scattering or Hoyle State properties

- Hoyle State
- Comparison



Hoyle State Comparison

	Exp ¹	Exp ²	Exp ³	FMD	α -cluster	'BEC' ⁴
$E(0_1^+)$	-92.16			-92.64	-89.56	-89.52
$E^*(2_1^+)$	4.44			5.31	2.56	2.81
$E(3\alpha)$	-84.89			-83.59	-82.05	-82.05
$E(0_2^+) - E(3\alpha)$	0.38			0.43	0.38	0.26
$E(0_3^+) - E(3\alpha)$	(3.0)	2.7(3)	3.96(5)	2.84	2.81	
$E(2_2^+) - E(3\alpha)$	(3.89)	2.6(3)	6.63(3)	2.77	1.70	
$r_{\text{charge}}(0_1^+)$	2.47(2)			2.53	2.54	
$r(0_1^+)$				2.39	2.40	2.40
$r(0_2^+)$				3.38	3.71	3.83
$r(0_3^+)$				4.62	4.75	
$r(2_1^+)$				2.50	2.37	2.38
$r(2_2^+)$				4.43	4.02	
$M(E0, 0_1^+ \rightarrow 0_2^+)$	5.4(2)			6.53	6.52	6.45
$B(E2, 2_1^+ \rightarrow 0_1^+)$	7.6(4)			8.69	9.16	
$B(E2, 2_1^+ \rightarrow 0_2^+)$	2.6(4)			3.83	0.84	

experimental situation
for 0_3^+ and 2_2^+ states
still unsettled

2_2^+ resonance at
1.8 MeV above
threshold included
NACRE compilation

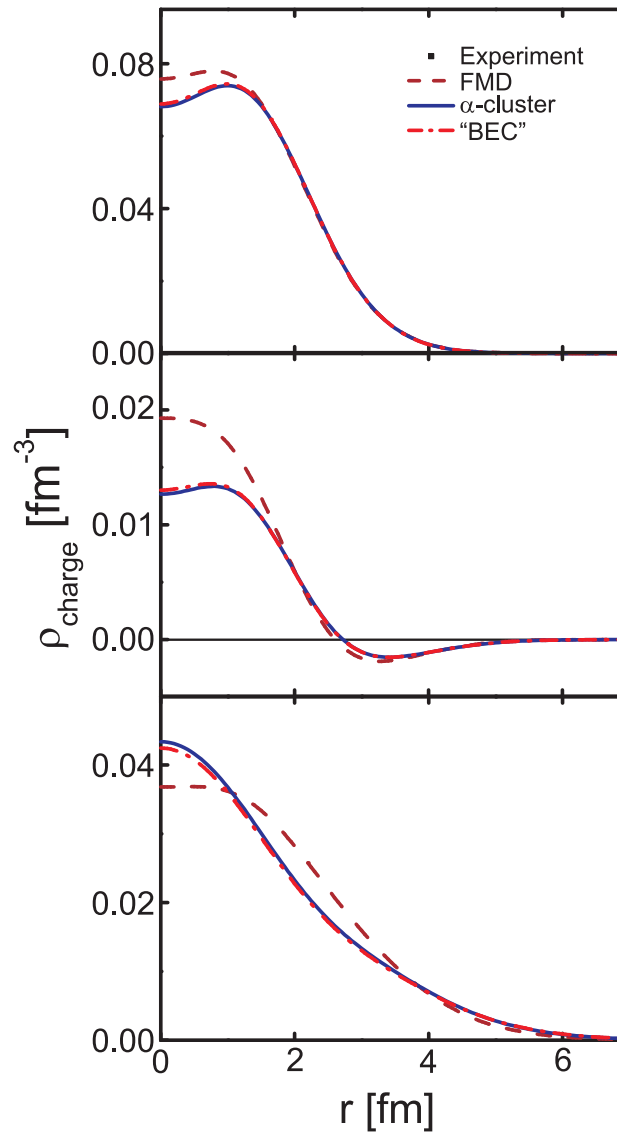
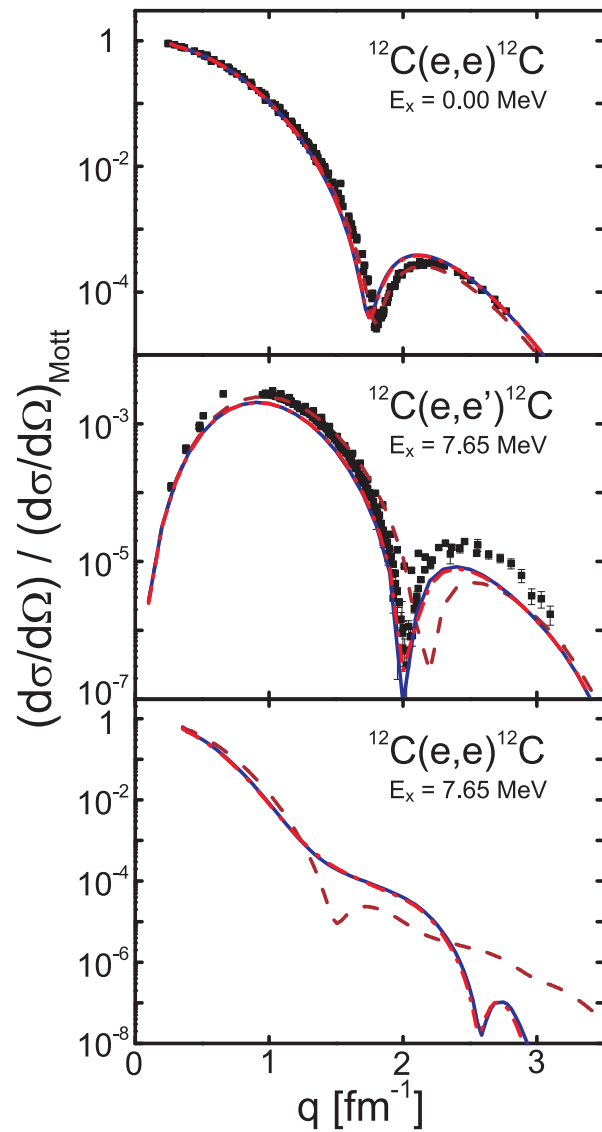
¹ Ajzenberg-Selove, Nuc. Phys. **A506**, 1 (1990)

² Itoh et al., Nuc. Phys. **A738**, 268 (2004)

³ Fynbo et al., Nature **433**, 137 (2005). Diget et al., Nuc. Phys. **A738**, 760 (2005)

⁴ Funaki et al., Phys. Rev. C **67**, 051306(R) (2003)

- Hoyle State
- Form factors and Densities



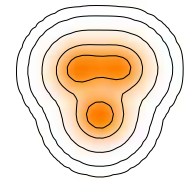
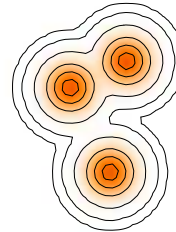
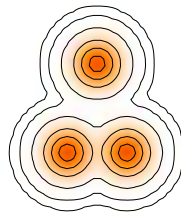
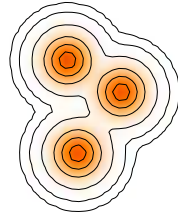
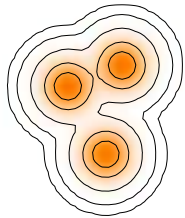
- compare with electron scattering data in Distorted Wave Born Approximation
- elastic form factor described very well by FMD
- transition form factor in first maximum better described by FMD, position of minimum and second maximum better described by cluster model

use intrinsic density

$$\rho(\mathbf{x}) = \sum_{k=1}^A \langle \Psi | \delta(\mathbf{x}_k - \mathbf{X} - \mathbf{x}) |$$

- Hoyle State
- Important Configurations

- Calculate the overlap with FMD basis states to find the most important contributions to the Hoyle state



$$|\langle \cdot | 0_1^+ \rangle| = 0.30$$

$$|\langle \cdot | 0_1^+ \rangle| = 0.25$$

$$|\langle \cdot | 0_1^+ \rangle| = 0.15$$

$$|\langle \cdot | 0_1^+ \rangle| = 0.08$$

$$|\langle \cdot | 0_1^+ \rangle| = 0.94$$

$$|\langle \cdot | 0_2^+ \rangle| = 0.72$$

$$|\langle \cdot | 0_2^+ \rangle| = 0.71$$

$$|\langle \cdot | 0_2^+ \rangle| = 0.61$$

$$|\langle \cdot | 0_2^+ \rangle| = 0.61$$

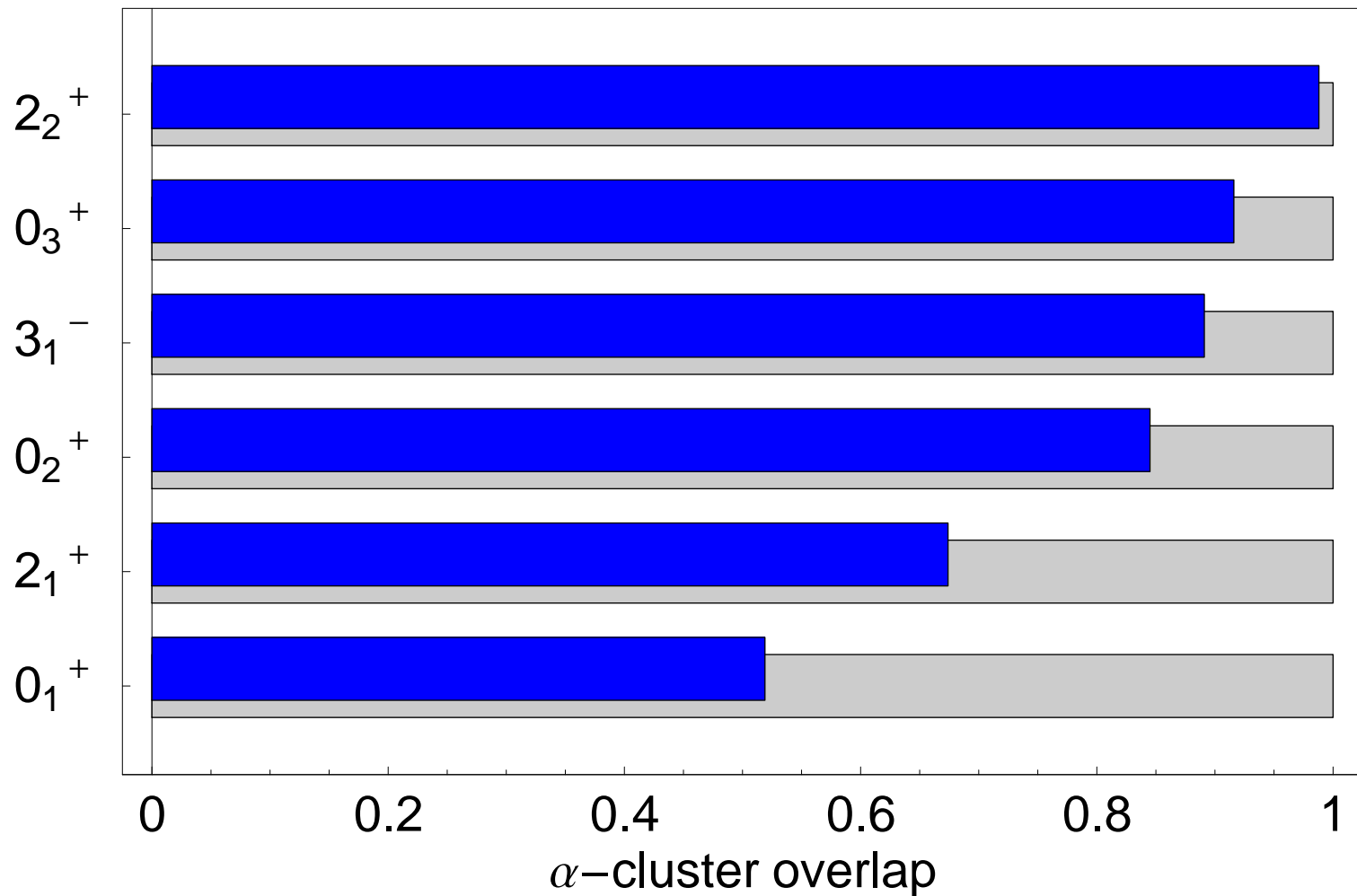
$$|\langle \cdot | 0_2^+ \rangle| = 0.04$$

FMD basis states are not orthogonal!

- Hoyle State
- **Overlap with Cluster Model Space**

Calculate the overlap of FMD wave functions with pure α -cluster model space

$$N_\alpha = \langle \Psi | P_{3\alpha} | \Psi \rangle$$

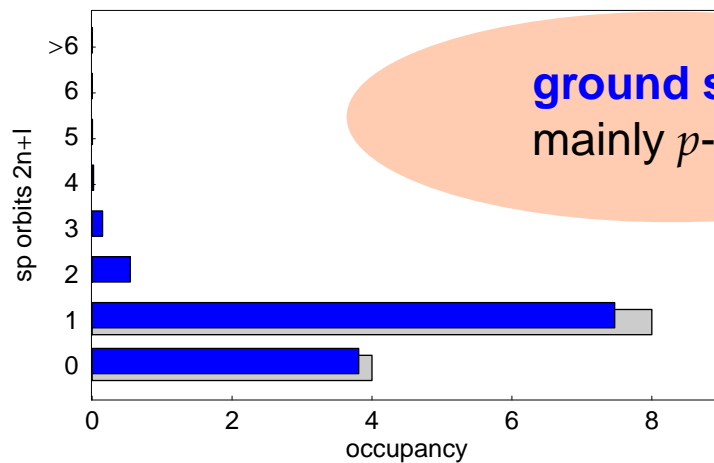


- Hoyle State
- Harmonic Oscillator Occupation Numbers

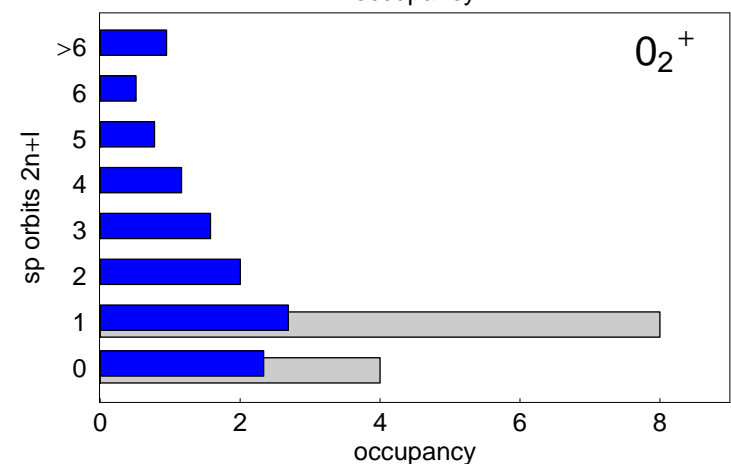
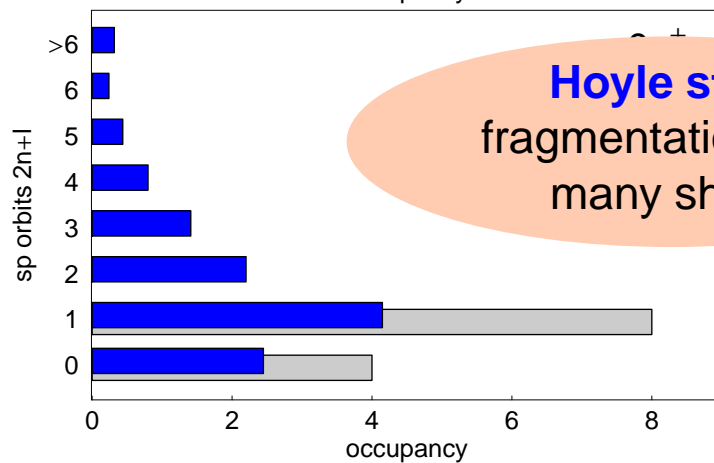
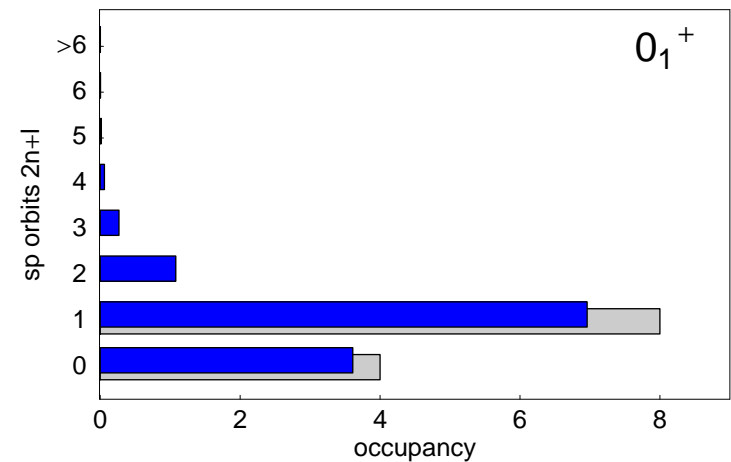
calculate one-body density in harmonic oscillator basis

$$n_{nlj} = \sum_m \langle \Psi | a_{nljm}^\dagger a_{nljm} | \Psi \rangle$$

FMD

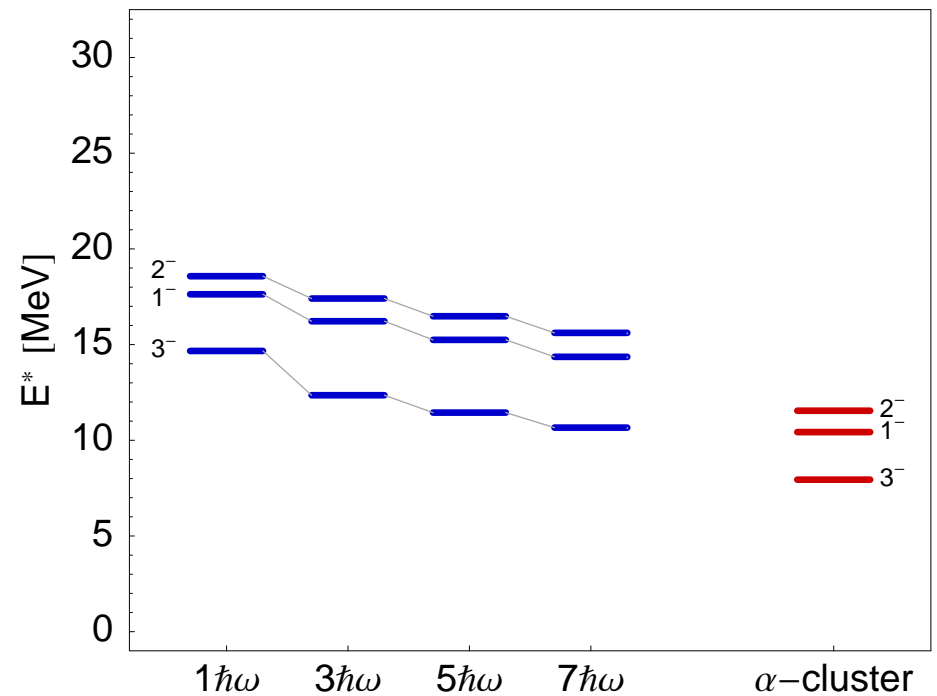
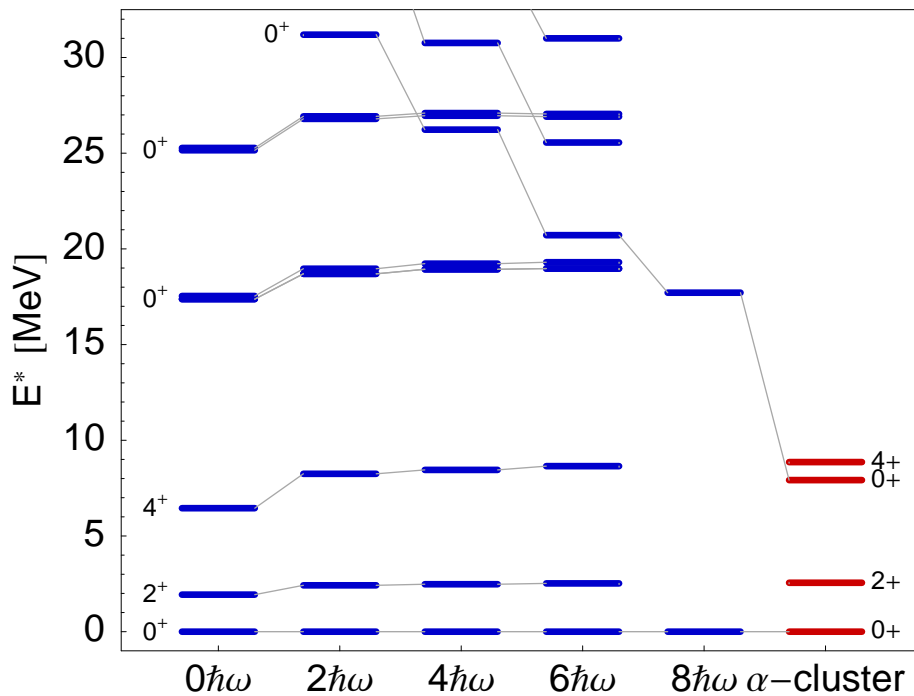


α -cluster



- Hoyle State
- α -cluster states in the No-Core Shell Model

- compare spectra in NCSM and α -cluster model using the Volkov interaction
- bare interaction used in NCSM calculations
- good agreement for ground state band (0_1^+ , 2_1^+ , 4_1^+)
- very slow convergence for cluster states



Fusion Cross Sections for Oxygen Isotopes



Astrophysical Motivation

Nuclear Structure

- Nucleus-Nucleus Interaction
- Map onto two-body problem
- Fusion Cross-Section

[nucl-th/0703030](#)

• **Pynconuclear Reactions**

- **pycnonuclear reactions** between neutron-rich isotopes are of importance for nucleosynthesis at **high density** in the deeper layers of accreting white dwarfs and neutron star envelopes
 - at these high densities (*pyknos* means compact, dense) the nuclei are positioned on a grid and the fusion cross section is enhanced because of **electron screening** effects
- FMD calculations provide an independent test for the cross-sections calculated with a Folding model

Michael Wiescher, Leandro R. Gasques

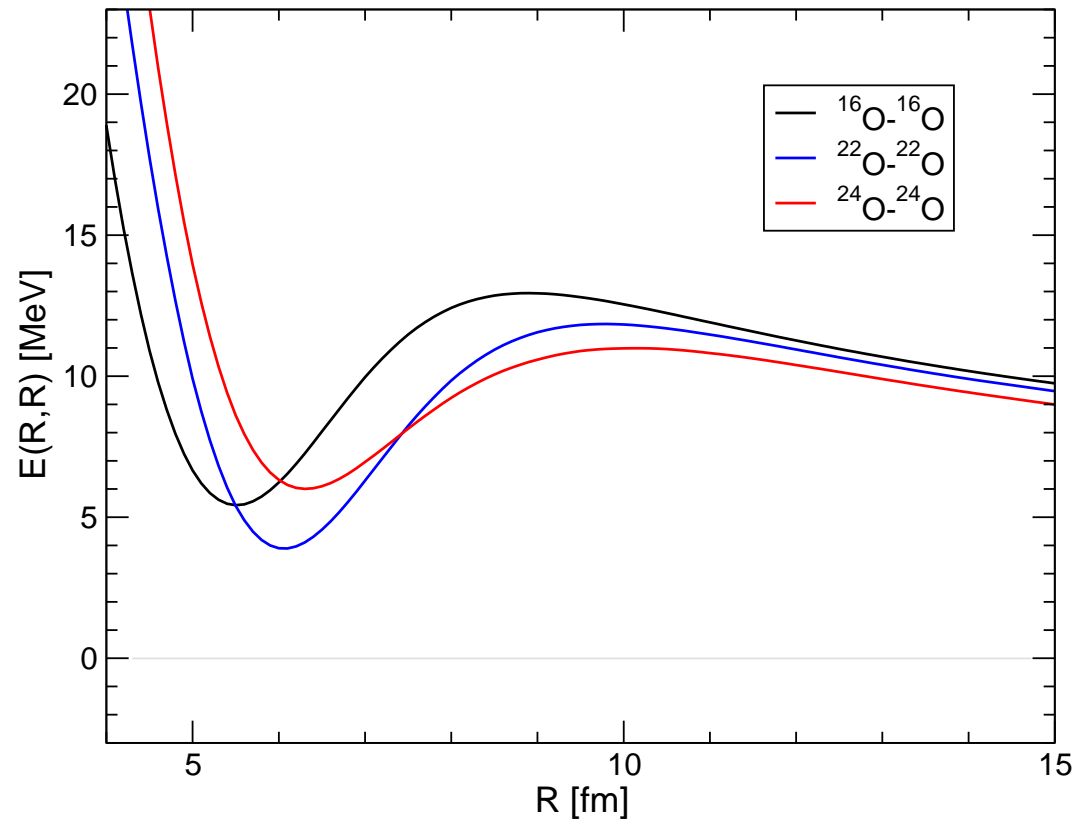
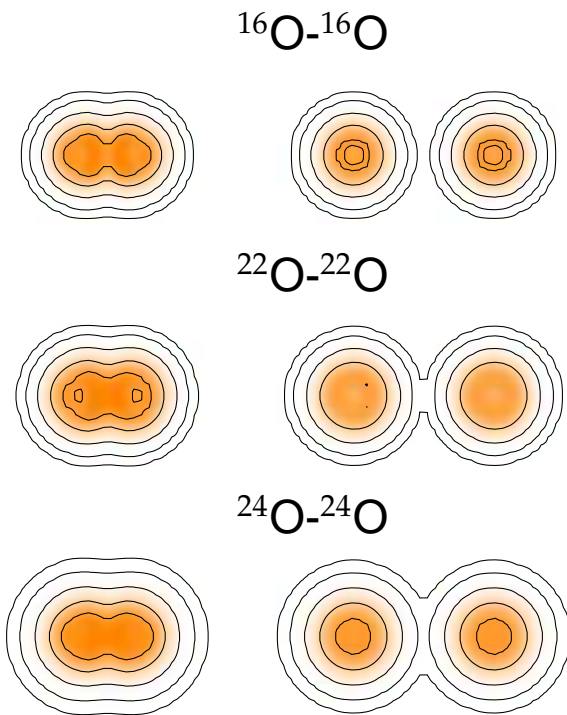
Nucleus-Nucleus Energy Surface

- calculate FMD ground states

- use GCM wave function $|\Psi(\mathbf{R})\rangle = \mathcal{A} \left\{ \left| \begin{smallmatrix} x\text{O}; \frac{1}{2}\mathbf{R} \end{smallmatrix} \right\rangle \left| \begin{smallmatrix} x\text{O}; -\frac{1}{2}\mathbf{R} \end{smallmatrix} \right\rangle \right\}$

- calculate GCM energy surface

$$E^L(R) = \frac{\langle \Psi(R\mathbf{e}_z) | (H - T_{\text{cm}}) P_{00}^L | \Psi(R\mathbf{e}_z) \rangle}{\langle \Psi(R\mathbf{e}_z) | P_{00}^L | \Psi(R\mathbf{e}_z) \rangle}$$



Map onto two-body system

- relative position of two clusters is smeared out in Slater determinant
- transform into RGM basis states
 $\phi(\xi)$ is internal wave function of oxygen nucleus

$$\langle \boldsymbol{\rho}, \xi_1, \xi_2 | \Phi(\mathbf{r}) \rangle = \mathcal{A} \{ \delta(\mathbf{r} - \boldsymbol{\rho}) \phi(\xi_1) \phi(\xi_2) \}$$

- if the same Gaussian width parameter a is used for all single-particle states is used, we can express the GCM state with the RGM basis states

$$|\Psi(\mathbf{R})\rangle = \int d^3r \Gamma(\mathbf{R} - \mathbf{r}) |\Phi(\mathbf{r})\rangle \otimes |\Phi_{\text{cm}}\rangle$$

with

$$\Gamma(\mathbf{R} - \mathbf{r}) = \left(\frac{\mu}{\pi a} \right)^{3/4} \exp\left(-\mu \frac{(\mathbf{R} - \mathbf{r})^2}{2a} \right), \quad \mu = \frac{A_1 A_2}{A_1 + A_2}$$

and the center-of-mass wave function

$$\langle \mathbf{X} | \Phi_{\text{cm}} \rangle = \left(\frac{A_1 + A_2}{\pi a} \right)^{3/4} \exp\left(-(A_1 + A_2) \frac{\mathbf{X}^2}{2a} \right)$$

- Fusion Cross Sections
- **Map onto two-body system**

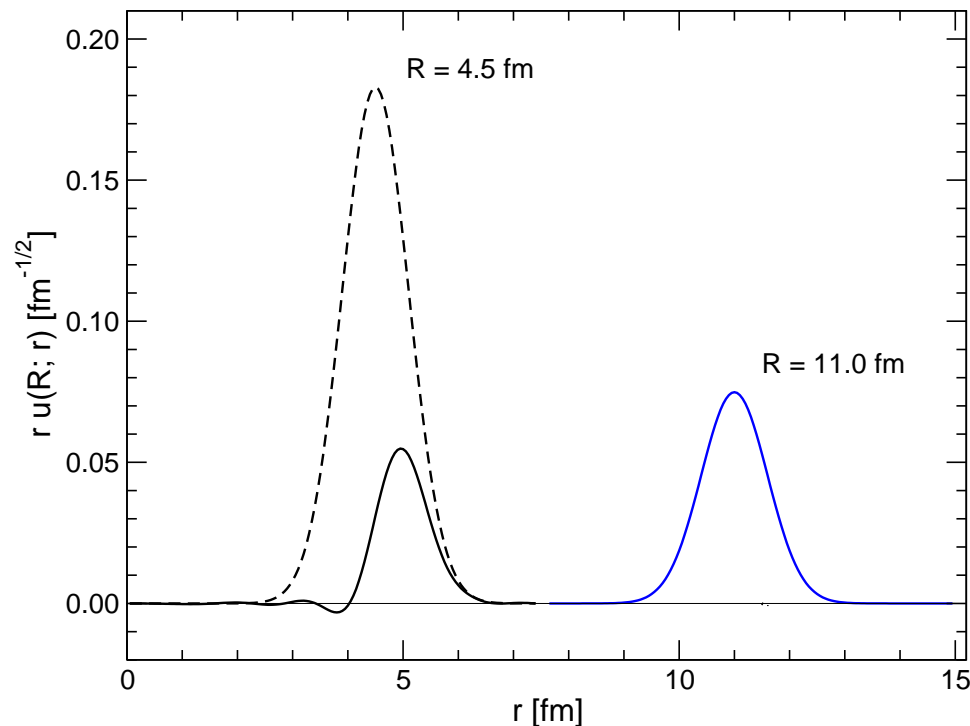
The RGM norm kernel is diagonal asymptotically

$$\langle \Phi(\mathbf{r}) | \Phi(\mathbf{r}') \rangle = n(\mathbf{r}, \mathbf{r}') \stackrel{r, r' \rightarrow \infty}{\equiv} [1 + \delta_{ab}(-1)^L] \delta(\mathbf{r} - \mathbf{r}')$$

- in order to map onto two-body system transform basis states diagonalize RGM norm kernel

$$|\tilde{\Phi}(\mathbf{r})\rangle = \int d^3r' |\Phi(\mathbf{r}')\rangle n^{-1/2}(\mathbf{r}', \mathbf{r}), \quad \langle \tilde{\Phi}(\mathbf{r}) | \tilde{\Phi}(\mathbf{r}') \rangle = [1 + \delta_{ab}(-1)^L] \delta(\mathbf{r} - \mathbf{r}')$$

- this procedure takes care of the **Pauli forbidden** states



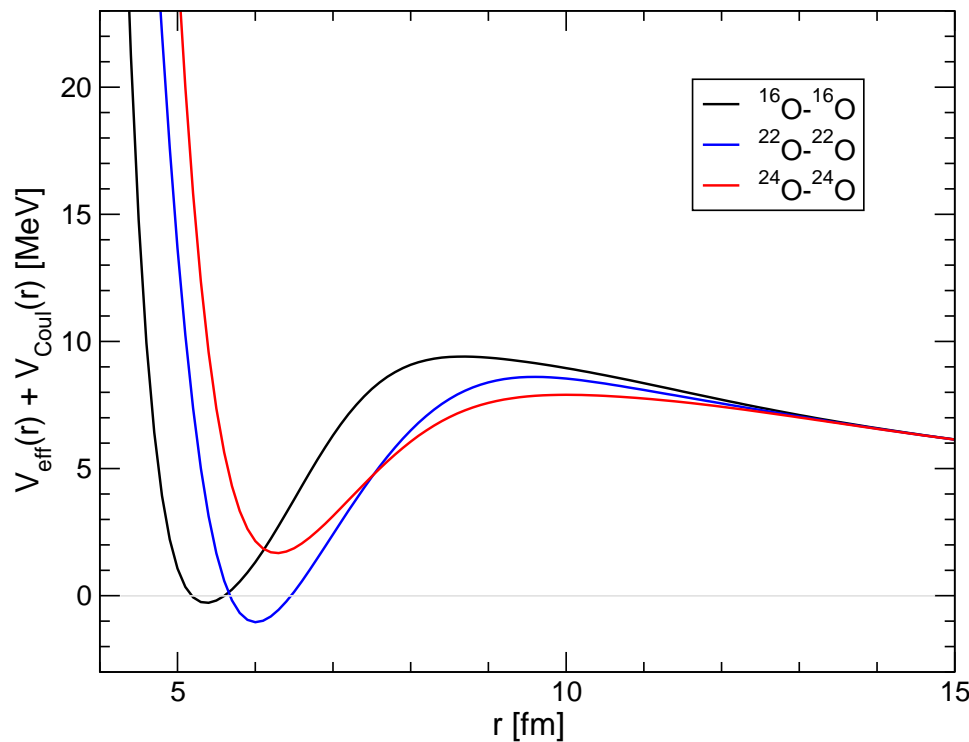
- Fusion Cross Sections
- Nucleus-Nucleus Potential

- Now fit a local effective potential to the GCM matrix elements

$$\langle \Psi(R_i \mathbf{e}_z) | P_{00}^L | \Psi(R_i \mathbf{e}_z) \rangle \stackrel{!}{=} \int dr r^2 \tilde{\Gamma}_L(R_i; r) \tilde{\Gamma}_L(R_i; r)$$

with

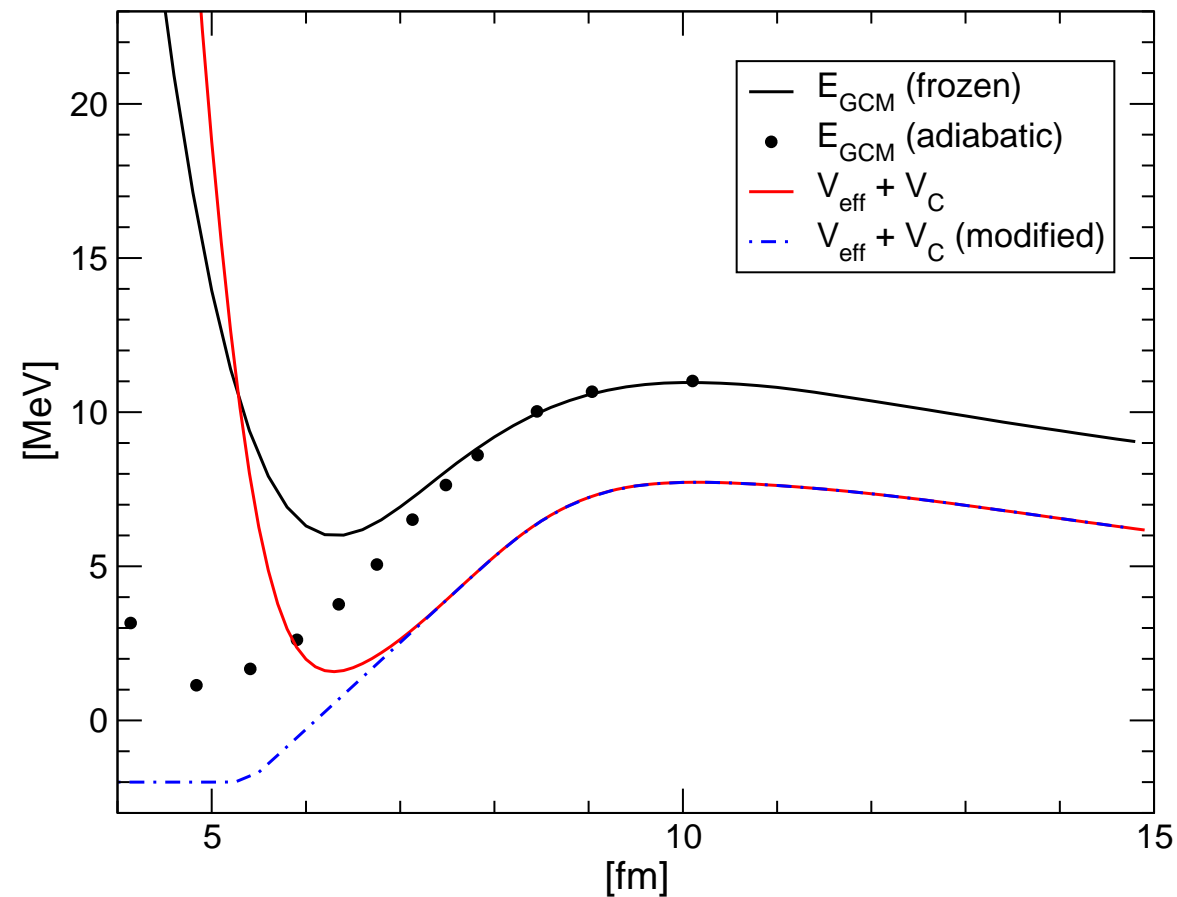
$$H_{\text{eff}}^L(r) = \frac{1}{2\mu m_N} p_{\text{rel}}^2 + \frac{L(L+1)}{2\mu m_N r^2} + V_{\text{eff}}^L(r) + V_C(r) + E_1 + E_2$$



fit turns out to be independent of L

- Fusion Cross Sections
- **Adiabatic Effects**

- estimate effects beyond the single-channel approximation
- adiabatic energy surface by constraining **quadrupole deformation** of system
- modify effective potential V_{eff} accordingly



Calculate Fusion Cross-Section

- solve two-body Schrödinger equation for all L with **Incoming Wave Boundary Condition** (assume that nuclei will fuse when the minimum of the potential is reached)

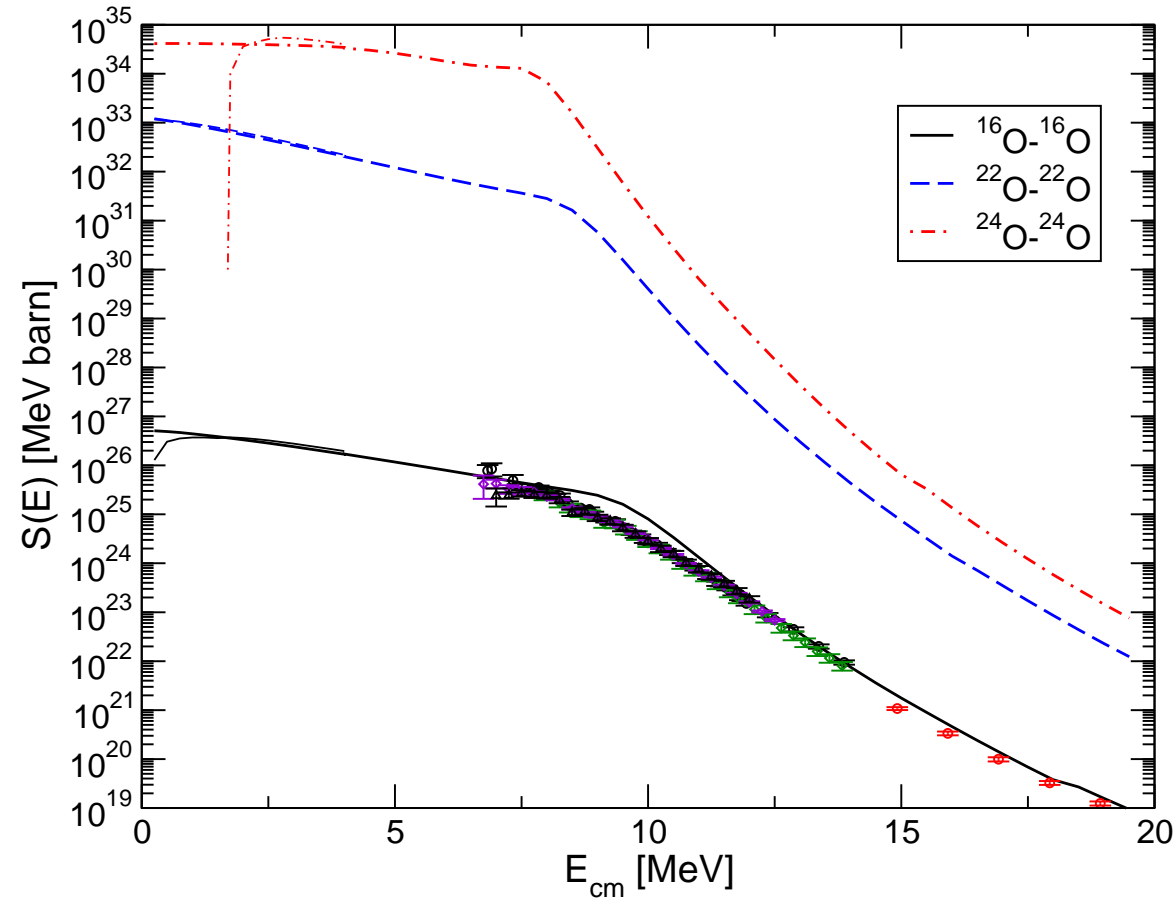
➔ therefore only real part of nucleus-nucleus potential is needed

- calculate and sum the penetration probabilities to calculate the fusion cross section

$$\sigma(E) = \frac{\pi}{k^2} \sum_{L=0}^{L_{crit}} [1 + \delta_{12}(-1)^L] (2L+1) P_L(E)$$

- convert into S-factor

$$S(E) = \sigma(E) E e^{2\pi\eta}$$



Radiative Capture



${}^3\text{He}(\alpha, \gamma){}^7\text{Be}$ reaction

- cluster model wave functions with FMD ground states
- improve description in the interaction region with FMD states for ${}^7\text{Be}$

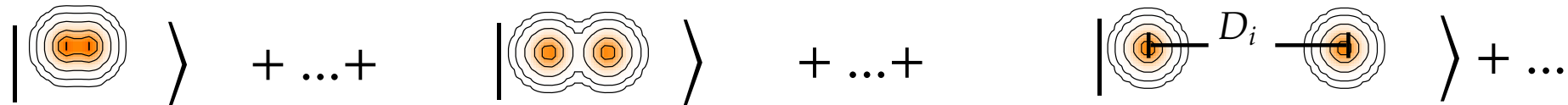
Program

- Implement boundary conditions
- Bound states, resonances and scattering states
- Capture cross section

- Radiative Capture
- Wave Functions



- asymptotic states like in a cluster model with FMD states for ${}^3\text{He}$ and ${}^3\text{He}$
- FMD states for ${}^7\text{Be}$ in the interaction region



Matching to the asymptotic solution

- for scattering and resonance states we have to implement **boundary conditions** by matching to the Coulomb solution of two point-like nuclei
- if the widths of all Gaussians are equal the relative motion of the two nuclei and the center of mass wave function is given analytically
- in the FMD we use a **projection on total linear momentum** to get rid of the center of mass problem and introduce a **collective variable representation** to access the relative wave function

- Radiative Capture
- **Collective-Coordinate Representation**

Size Measure

➔ Operator \tilde{B} measures extension of the system

$$\tilde{B} = \frac{1}{A^2} \sum_{i < j=1}^A (\tilde{x}(i) - \tilde{x}(j))^2$$

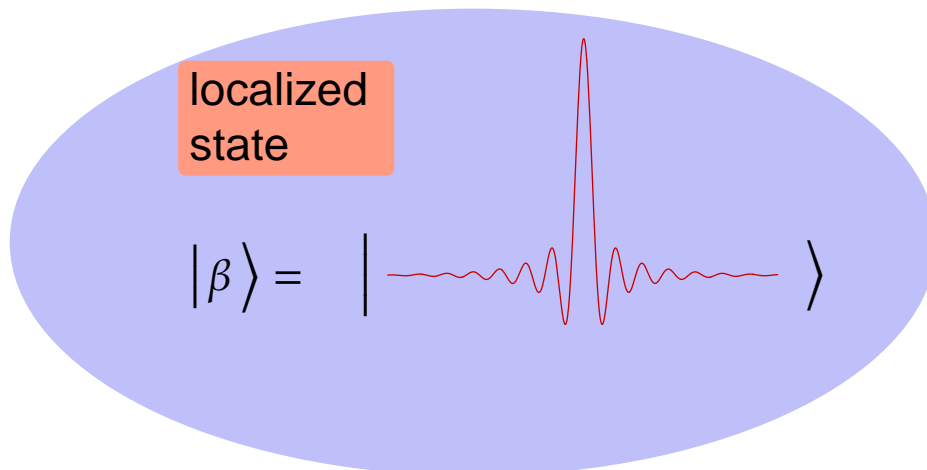
Asymptotic Interpretation

➔ Eigenvalues relate to relative distance r

$$\tilde{B}|\beta\rangle = \beta|\beta\rangle \Rightarrow \beta(r) = \frac{A_1 A_2}{A^2} r^2 + \beta_1 + \beta_2$$

➔ Eigenvectors localize in r (localized states)

$$\langle \beta | \tilde{B}^2 | \beta \rangle = \langle \beta | \tilde{B} | \beta \rangle^2$$



➔ Identify Collective Wave Function

$$\Psi(r(\beta)) := \frac{1}{\sqrt{\Delta}} \langle \beta | \Psi \rangle$$

• Radiative Capture

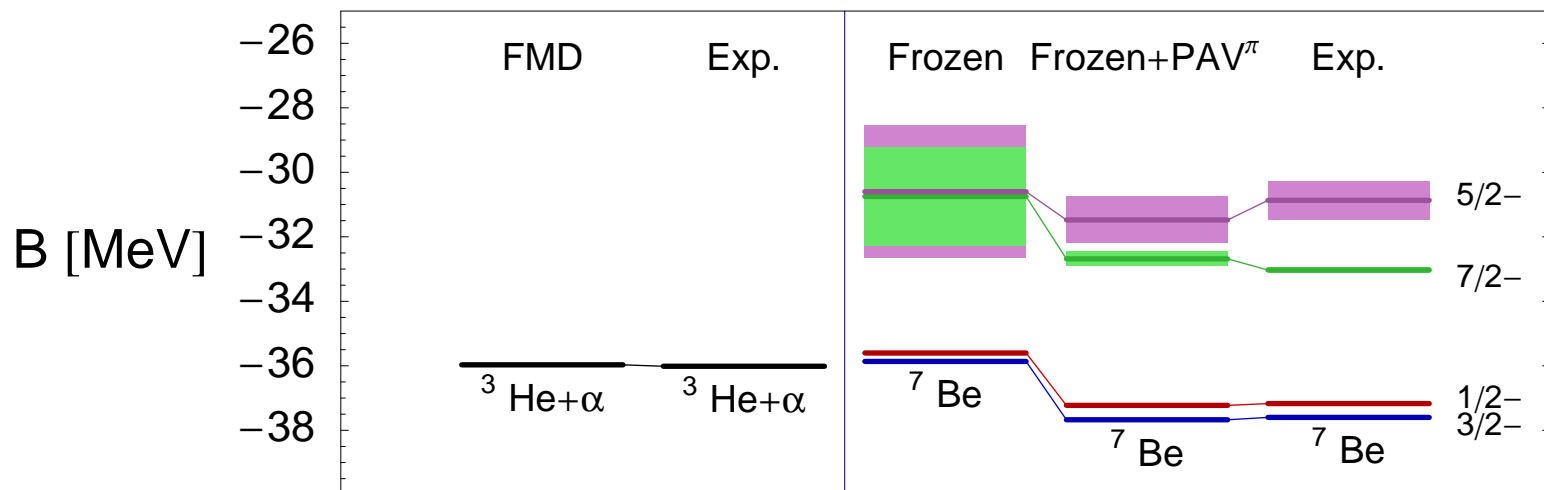
• ⁷Be Bound states and Resonances

- calculate bound states by matching RGM wave function to Whittaker function

$$u_L(r) \propto W_{-\eta, L+\frac{1}{2}}(2kr)/(kr), \quad k = \sqrt{-2\mu E}, \eta = (\mu Z_1 Z_2 e^2)/k$$

- calculate resonances by matching to purely outgoing Coulomb solution (Gamow boundary conditions), complex eigenvalue $E_{\text{res}} + \frac{i}{2}\Gamma$

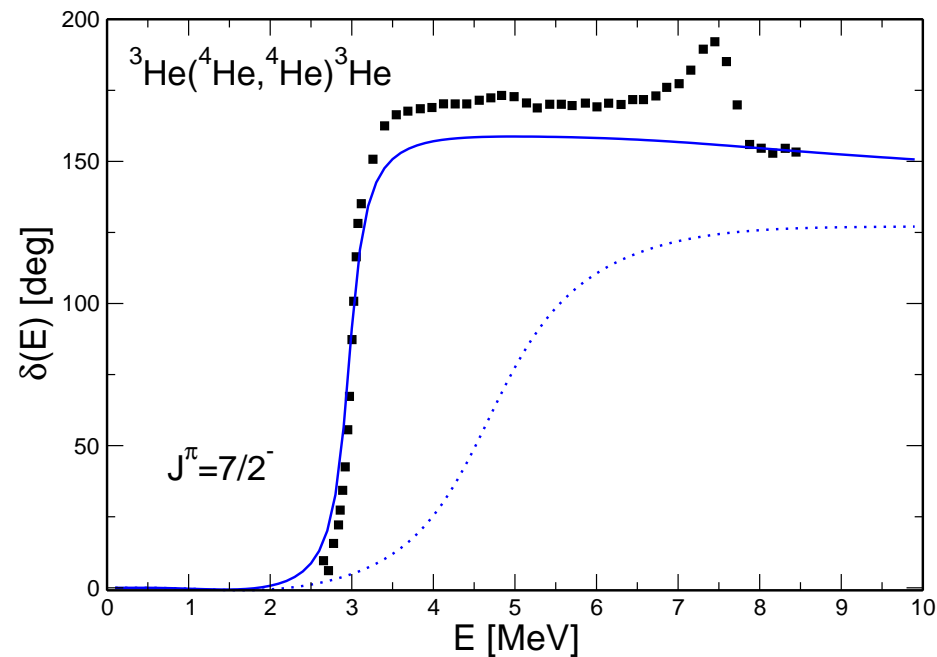
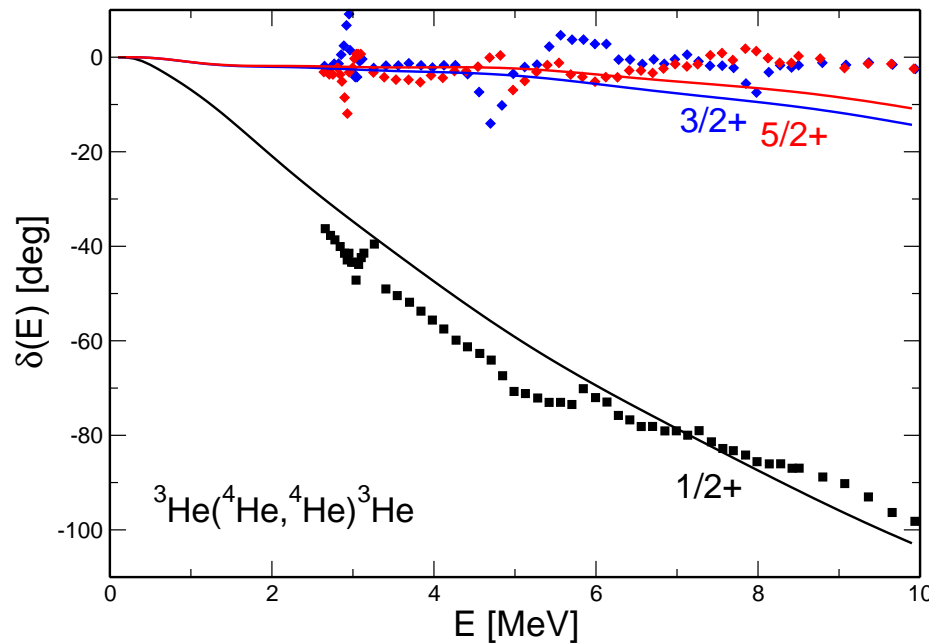
$$u_L(r) \propto [G_L(\eta, kr) + iF_L(\eta, kr)], \quad k = \sqrt{2\mu E}$$



- Radiative Capture
- $^3\text{He}-^4\text{He}$ Phaseshifts

- determine scattering solutions by matching to Coulomb solutions
unit flux scattering wave function

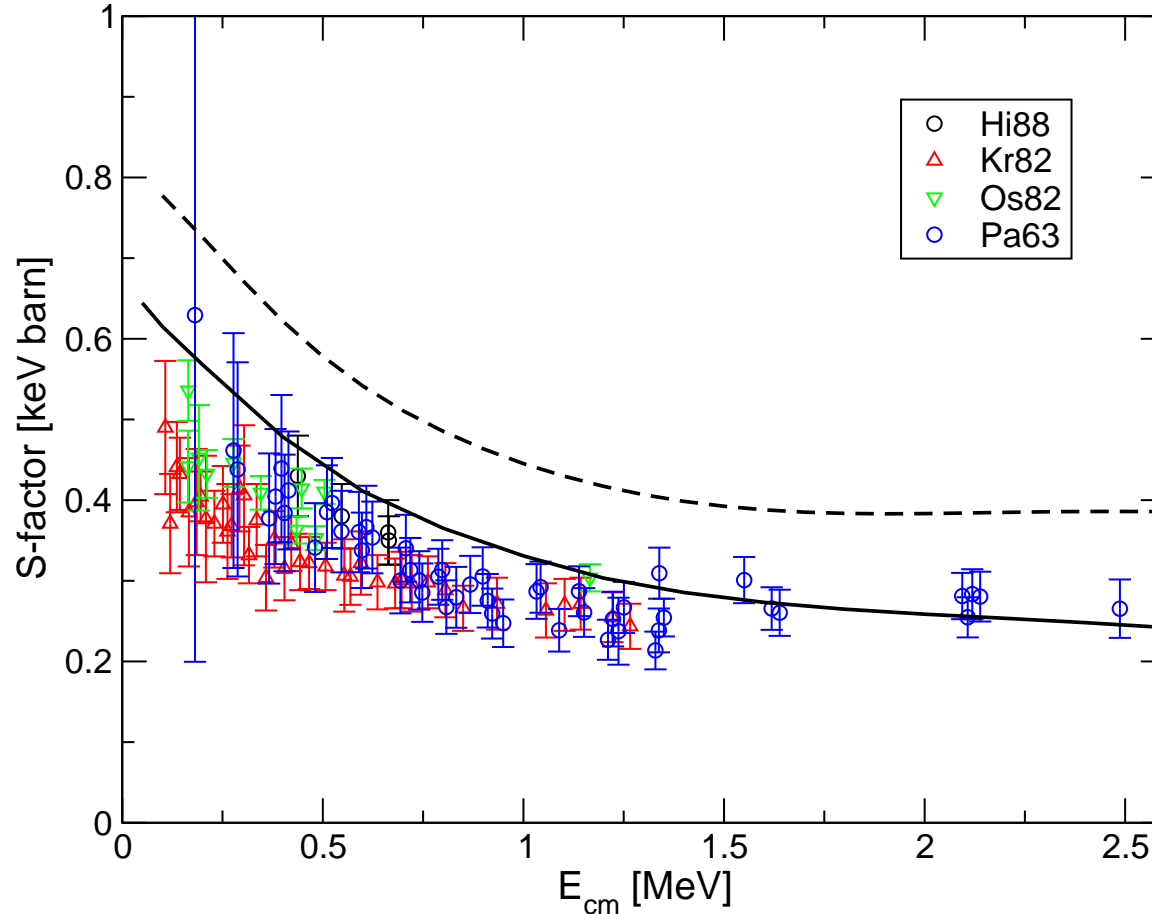
$$\langle \mathbf{r} | \Psi \rangle = \frac{1}{\sqrt{v}} \sum_L \sqrt{4\pi} \sqrt{2L+1} i^L e^{i\sigma_L} [F_L(\eta, kr) + \tan(\delta) G_L(\eta, kr)] Y_{L0}(\hat{r}) / (kr)$$



Radiative Capture S-Factor

preliminary

- Capture from $1/2^+$, $3/2^+$ and $5/2^+$ scattering states into $3/2^-$ and $1/2^-$ bound states
- S-Factor for ${}^7\text{Be}$ described in the interaction region by single PAV^π configuration (dashed line) or VAP configurations for $3/2^-$ and $1/2^-$ (solid line)



Summary

Unitary Correlation Operator Method

- explicit description of short-range central and tensor correlations
- phase-shift equivalent correlated interaction V_{UCOM}

Fermionic Molecular Dynamics

- Structure of light nuclei
- Halos and clustering

Cluster Degrees of Freedom

- GCM cluster states naturally described in FMD
- RGM wave function needed to implement boundary conditions for scattering or resonance states
- use for fusion and radiative capture reactions

Collaborators

- A. Cribeiro, R. Cussons, **H. Feldmeier**, K. Langanke, R. Torabi
GSI Darmstadt
- H. Hergert, N. Paar, P. Papakonstantinou, **R. Roth**
Institut für Kernphysik, TU Darmstadt